DISSERTATION

on

MODELLING AND EXPERIMENTAL ANALYSIS OF A THERMAL SYSTEM EQUIVALENT TO A CAR PARKED IN DIRECT SUNLIGHT

Submitted in partial fulfilment of the requirement for the award of degree of

Master of Engineering

IN

CAD/CAM Engineering

Submitted By

Sushank Dixit

Roll No. 801281007

Under the Supervision of

Dr. Tarun Kumar Bera

and

Mr. Devender Kumar

Assistant Professor
Department of Mechanical Engineering
Thapar University,
Patiala

DEPARTMENT OF MECHANICAL ENGINEERING
THAPAR UNIVERSITY
PATIALA-147004, INDIA
JULY 2014

DECLARATION

I hereby declare that the seminar report entitled **"Modelling and Experimental Analysis of a Thermal System Equivalent to a Car Parked in Direct Sunlight"** in the partial fulfilment for award of degree of **Master of Engineering** submitted in **Department of Mechanical Engineering, Thapar University, Patiala,** is a record of my own work carried out under the supervision and guidance of **Dr. T. K. Bera** and **Mr. Devender Kumar, Assistant Professor, Department of Mechanical Engineering, Thapar University.** This matter embodied in this report has not been submitted in part or full to any other university or institute for the award of any degree.

(Sushank Dixit)

This is to certify that above declaration made by the student concerned is correct to the best of my knowledge & belief.

Mr. Devender Kumar
Assistant Professor
Thapar University, Patiala

Dr. Tarun Kumar Bera
Assistant Professor
Thapar University, Patiala

Countersigned by:

Head of ME Department
Thapar University, Patiala

Dean of Academic Affairs
Thapar University, Patiala

ii

ACKNOWLEDGEMENT

My foremost and profound gratitude goes to my guides Dr. T. K. Bera and Mr. Devender Kumar for their proficient, enthusiastic guidance and encouragement. The suggestions given by them undoubtedly helped in supplementing my thoughts in the right direction for attaining the desired objectives.

My heartfelt gratitude goes to Dr. Ajay Batish, Professor and Head, MED, for providing all the facilities required for completion of this work.

I am also thankful to all the teaching and non-teaching staff members of mechanical engineering department who have contributed directly or indirectly towards the successful completion of this thesis.

I would like to thank, all my friends of Thapar University for their love, care, help and support.

Most significantly, none of this would have been possible without the love and patience of my family. My parents to whom this dissertation is dedicated to, has been a relentless supply of love, concern, support and strength for these years.

All above, I express my indebtedness to the "ALMIGHTY GOD" for all His blessings and kindness.

Sushank Dixit

Roll No. 801281007

ABSTRACT

This thesis is to determine the amount of heat getting accumulated in the interior of a car. For this purpose, a box is made up of toughened glass and it is to be used to check the amount of heat getting accumulated into the box. At the later stage, a double layer box is made up of toughened glass and air is filled in between the two layers of glasses. The amount of heat getting accumulated in the interior of the glass cabin is measured. In the third stage, instead of air, argon gas is used in between the two layers of glasses in such a way that it cannot escape. Now, again the amount of heat accumulated in the interior of the double layer glass cabin is measured. In the next phase, instead of trapped argon, flowing argon is used in between the two layers of toughened glasses and temperature of the air present inside the closed cabin is measured. The bond graph model of the entire thermal system with single and double layers of glasses is developed. For the validation, the results obtained from the experiments are compared with the results from the Bond graph modelling and it is observed that the theoretical results closely match with the experimental results.

Keywords: System, Car Cabin, Thermal Analysis, Experimental Analysis, Bond Graph Modelling, Toughened Glass, Argon Gas, Double Layer Glass Box.

LIST OF ABBREVIATIONS

C	Capacitance
CIP	Cast in Place
De	Effort Detector
Df	Flow Detector
GY	Gyrator
I	Inertia
PVB	Poly-Vinyl Butyral
R	Resistance
SE	Source of Effort
SF	Source of Flow
ST	Surrounding Temperature
SRCCT	Simulation Result Central Cabin Temperature
SROGT	Simulation Result Outer Glass Temperature
SRIGT	Simulation Result Inner Glass Temperature
SRATT	Simulation Result Air Trapped Temperature
SRTAT	Simulation Result Trapped Argon Temperature
UVC	Ultra-Violet C
UVB	Ultra-violet B
UVA	Ultra-violet A
Y	Solar Heat Flux

NOMENCLATURE

a_g	Absorptivity of Glass
a_{ar}	Absorptivity of Argon Gas
a_a	Absorptivity of Air
A	Area
C_g	Specific Heat of Glass
C_{ar}	Specific Heat of Argon
C_{air}	Specific Heat of Air
e_g	Emissivity of Glass
e_{ar}	Emissivity of Argon Gas
e_{air}	Emissivity of Air
h_{ar}	Convective Heat Transfer Coefficient of Argon Gas
h_{air}	Convective Heat Transfer Coefficient of Air inside the Cabin.
h_{ca}	Convective Heat Transfer Coefficient of outside Air
I_r	Irradiance
K	Compliance Element
m_g	Mass of Glass
m_{ar}	Mass of Argon present in between Two Glass
m_{air}	Mass of Air inside the Cabin
Q_{tg}	Heat Transmitted by Glass
Q_{ag}	Heat Absorbed by Glass
Q_{ag2}	Heat Absorbed by outer Glass
Q_{ag1}	Heat Absorbed by inner Glass
Q_{tg1}	Heat Transmitted by inner Glass
Q_{ra}	Radiative Heat Transfer
Q_{ca}	Convective Heat Transfer
Q_{aa2}	Heat Absorbed by Air present in between Two Glass
Q_{aar}	Heat absorbed by the Argon Gas present in between Two Glass
r_g	Reflectivity of Glass

R_{ca}	Convective Thermal Resistance
R_{ra}	Radiative Thermal Resistance
t_g	Transmissivity of Glass
T_{ga}	Glass Temperature
T_{ga2}	Temperature at outer Glass
T_{ga1}	Temperature of inner Glass
T_{a1}	Atmospheric Temperature
T_{aa}	Inside Air Temperature
T_{aa2}	Temperature of Atmospheric Air present in between Two Glass
T_s	Temperature of Space
σ	Stefan Boltzmann Constant

LIST OF FIGURES

Figure No.	Title	Page No.
1.1	Windshield of a car	5
1.2	Side glass of a car	6
3.1	Bond Graph representation of compliance element	19
3.2	Bond Graph representation of resistive element	20
3.3	Bond Graph representation of inertial element	20
3.4	Bond Graph representation of source of effort element	21
3.5	Bond Graph representation of source of flow element	21
3.6	Bond Graph representation of transformer element	22
3.7	Bond Graph representation of gyrator element	22
3.8	Bond Graph representation of 0-junction	23
3.9	Bond Graph representation of 1-junction	23
3.10	Causality concept	25
3.11	Causality of source of effort	26
3.12	Causality of source of flow	26
3.13	Integral causality of inertial element	26
3.14	Integral causality of compliant element	27
3.15	Causality of resistive element	27
3.16	Causality of transformer element	27
3.17	Causality of gyrator element	28
3.18	Causality of 0-junction	28
3.19	Causality of 1-junction	29
3.20	Causality of 1-junction	30
3.21	Bond Graph model of single glass layer	30
3.22	Simulation results of single layer glass	35
3.23	Bond Graph of double glass layer with air trapped condition	36
3.24	Simulation results of double layer glass with air trapped	43
3.25	Double layer glass cabin, argon trapped condtion	44
3.26	Bond Graph of double layer glass with trapped argon	44
3.27	Simualtion result of double layer glass with trapped argon	51
3.28	Bond Graph of double layer glass with flowing argon	51
3.29	Simulation result of double layer glass cabin with flowing argon	58

4.1	Glass supporting structure	60
4.2	Thermocouple	61
4.3	Digital thermometer	61
4.4	Argon gas cylinder	62
4.5	Solar power meter	63
4.6	Cabin made up of single glass layer	64
4.7	Experimental results of single layer glass cabin	65
4.8	Double layer glass cabin with trapped air	66
4.9	Experimental results of double layer glass with trapped air	67
4.10	Glass separated by separator	68
4.11	Argon-oxygen separator	69
4.12	Cabin of double glasses with trapped argon	70
4.13	Experimental results of double layer glass cabin with trapped argon	71
4.14	Cabin of double glasses with flowing argon	72
4.15	Experimental results of double layer glass cabin with flowing argon	73
4.16	Experimental results v/s simulation results of single layer glass	74
4.17	Experimental results v/s simulation results of double layer glass with trapped air.	76
4.18	Experimental results v/s simulation results of double layer glass with trapped argon.	77
4.19	Experimental results v/s simulation results of double layer glass with flowing argon.	78

LIST OF TABLES

Table No.	Title	Page No.
3.1	Power variables in different energy domains	18
3.2	Bond Graph element	24
3.3	Parameter values for single layer glass cabin	33
3.4	Simulation results of single layer glass cabin	34
3.5	Parameter values for double layer glass cabin, air trapped condition	41
3.6	Simulation results of double layer glass cabin, air trapped condition	42
3.7	Parameter values for double layer glass cabin, argon trapped condition	49
3.8	Simulation results of double layer glass cabin, argon trapped condition	50
3.9	Parameter values for double layer glass cabin, argon flowing condition	56
3.10	Simulation results of double layer glass cabin, argon flowing condition	57
4.1	Experimental results of single layer glass cabin	64
4.2	Experimental results of double layer glass cabin, air trapped condition	67
4.3	Experimental results of double layer glass cabin, argon trapped condition	70
4.4	Experimental results ofdouble layer glass cabin, argon flowing condition	72
4.5	Results of single layer glass cabin	74
4.6	Results of double layer glass, air trapped condition	75
4.7	Results of double layer glass cabin, argon trapped condition	76
4.8	Results of double layer glass cabin, argon flowing condition	77

TABLE OF CONTENTS

CERTFICATE i

DECLARATION ii

ACKNOWLEDGEMENT iii

ABSTRACT iv

LIST OF ABBREVATIONS v

NOMENCLATURE vi

LIST OF FIGURES viii

LIST OF TABLES x

CHAPTER1: INTRODUCTION 1–9

1.1 Background and Motivation 1

1.2 Solar Heat Waves 1

1.2.1 Direct Solar Radiation 2

1.2.2 Indirect Solar Radiation2

1.3 Glasses 3

1.3.1 Manufacturing of Glass 3

1.3.2 Toughened Glass 3

1.3.3 Laminated Glass 4

1.4Windshield 5

1.5 Side Glass 6

1.6Modes of Heat Transfer6

1.7Contribution of Thesis 8

1.8Organization of Thesis 9

CHAPTER 2: LITERATURE REVIEW10–16

2.1 Introduction 10

2.2 Cooling Energy Efficiency and Solar Radiation Effect on a System 10

2.3 Heat Flow Analysis using Bond Graph 15

2.4 Literatures Gap 16

2.5 Objective of the Work 16

CHAPTER 3: MODELLING THE COOLING EFFECT OF A SYSTEM EQUIVALENT TO A CAR17–57

3.1 Introduction17

3.2 Bond Graph Modelling17

3.2.1 Bond Graph Standard Element18

3.2.2 Basic 1-Port Element19

3.2.3 Basic 2-Port Element21

3.2.4 Junction23

3.2.5 Causality 25

3.3 Thermal Modelling of the System Surrounded by a Single Layer of Glass 29

3.3.1Parameter Values 33

3.3.2 Simulation Results 34

3.4 Thermal Modelling of the System Surrounded by Double Layer of Glass with Air between Two Glasses 35

3.4.1Parameter Values 41

3.4.2 Simulation Results 42

3.5 Thermal Modelling of the System Surrounded by Double Layer of Glass with Argon between Two Glasses 43

3.5.1Parameter Values 49

3.5.2 Simulation Results 50

3.6 Thermal Modelling of the System Surrounded by Double Layer of Glass with Flowing Argon between Two Glasses 51

3.6.1Parameter Values 56

3.6.2 Simulation Results 57

CHAPTER 4: EXPERIEMENTAL PROCEDURE59–77

4.1 Introduction 59

4.2 Selection of Material 59

4.2.1 Wood 59

4.2.2Toughened Glass 60

4.2.3Thermocouple and Digital Thermometer 60

4.2.4Argon Gas62

4.2.5Solar Power Meter 62

4.2.6Pipes and Connector 63

4.3 Experimentation on the System Surrounded by a Single Layer of Glass 63

4.3.1 Experimental Results 64

4.4 Experimentation on the System Surrounded by Double Layer of Glass with Air between Two Glasses 65

4.4.1 Experimental Results 66

4.5 Experimentation on the System Surrounded by Double Layer of Glasswith Argon between Two Glasses 68

4.5.1 Experimental Results 70

4.6 Experimentation on the System Surrounded by Double Layer of Glass with Flowing Argon between Two Glasses71

4.6.1 Experimental Results 72

4.7Validation with the Theoretical Results73

4.7.1 Validation of Single Layer Glass Cabin73

4.7.2Validation of Double Layer Glass Cabin with Air in between Two Glasses 75

4.7.3Validation of Double Layer Glass Cabin with Argon in between Two Glasses . 76

4.7.4Validation of Double Layer Glass Cabin with Argon Flowing in between Two Glass 77

CHAPTER 5: CONCLUSION 79

5.1 Conclusion79

5.2Scope of Future Work79

REFRENCES80

CURRICULUM VITAE82

CHAPTER 1 INTRODUCTION

Summer is the warmest of all four seasons; it falls between spring and autumn. During summer season the temperature of the environment is very high and it generally varies between 40^0C to 50^0C. If a vehicle is parked in such a high temperature, heat gets accumulated in the vehicle. The solar heat waves enter in the interior of the vehicle from many sources such as windshield, roof, side window glass and rear window glass. This causes the temperature to rise in the vehicle and this rise is nearly 20^0C to 30^0C more than that of the atmospheric temperature. This rise in temperature is unbearable for the passengers of the car and it also affects the electronic components present in the car.

1.1 Background and Motivation

When a car is parked in direct sunlight, the heat waves from the sun enter into the car's interior through windshield, roof, side window glass and rear window glass. These heat waves get trapped into the car's interior compartment due to change in wavelength and eventually increase the temperature of the car cabin. This temperature rise is so high that it gets unbearable for the passengers of the car.

So, the main objective of this work is to reduce the temperature of the interior of the car. This can be done by using two layers of glasses as a windshield instead of single layer and flowing some sort of gasses between the two glasses so as to reduce the heat accumulation.

1.2 Solar Heat Waves

Almost all the energy required for driving various systems such as climate-system, ecosystem, hydro system *etc*. are obtained from the sun. The solar energy is created at the centre of the sun during nuclear fusion. In nuclear fusion, the hydrogen atom is fused into the helium atom and the energy is generated. The surface temperature of the sun is about 5800 K and the total energy emitted by the sun is about 6,30,00,000 Watt/m^2 .

The sun emits electromagnetic radiations in the form of gamma rays. These gamma rays consist of high energy photon and before reaching to the sun-surface it gets converted to low energy photon. Thus, the sun does not emit the gamma rays but it definitely emits X-rays, ultra-violet rays, visible, infrared and also radio waves.

The solar electromagnetic radiation that reaches the earth atmosphere has a spectral span of 100 nm to 1 mm. The electromagnetic rays emitted by the sun are as follows:

- **Ultra-violet C (UVC):** The ultra-violet C has a spectral range between 100−280 nm. The name ultra-violet refers to the fact that the radiations are emitted at a frequency, higher than that of the violet light and thus, it is not visible to human eye. As most of the ultra-violet radiations are absorbed by the atmosphere, a very little amount of ultra-violet radiation reach to the earth surface.
- **Ultra-violet B (UVB):** It has a spectral range of 280−315 nm. As like UVC, most of UVB also gets absorbed by the atmosphere. It causes sunburn and also damages the DNA.
- **Ultra-violet A (UVA):** It has a wavelength range of 315−400 nm. Previously it was thought that these rays do not affect the DNA and thus it was used in cosmetic artificial sun-tanning but later, it was found that it damages the DNA in an indirect way (formation of free radicals and reactive oxygen species). It also causes cancer.
- **Visible Light:** It has wavelength range of 380−780 nm. It is visible to the naked eye. Out of the total radiation coming from the sun, most are in the visible range.
- **Infrared:** It has a spectral range of 700−1 mm. After the visible light, it is the second largest content of the electromagnetic radiation coming from the sun. It is further divide into 3 types depending on the wavelength *i.e.*,
    - Infrared A: 700−1400 nm
    - Infrared B: 1400−3000 nm
    - Infrared C: 3000−1 mm

1.2.1 *Direct Solar Radiation*

The direct normal radiation is the amount of solar radiation received by the surface per unit area, which is always perpendicular to ray of the light. In a clear sunny day, most of the light coming from the sun is in the form of direct solar radiation.

1.2.2 *Indirect (Diffused) Solar Radiation*

In diffused solar radiation, the ray of light coming from the sun does not come in a straight line. It gets scattered due to the particles and molecules present in the atmosphere but comes equally from all directions. In cloudy days, most of the solar radiation coming from the sun, comes in the form of diffused solar radiation.

1.3 Glasses

Most of the glasses are silicate glasses. They are transparent and are not affected by chemicals. Today glasses are available in different forms depending upon their use. Different processes were performed on the glass, so as to make it useful for a particular application.

The major constituents in manufacturing of glass are

- Limestone ($CaCO_3$)
- Soda ash (Na_2CO_3)
- Sand (SiO_2)

1.3.1 *Manufacturing of Glass*

Limestone ($CaCO_3$), sand (SiO_2) and soda ash (Na_2CO_3) are mixed properly and are poured into a tank-furnace. Then it is heated to a temperature of about 1700^0 C. The tank is made shallow at one end and deeper at the other end, so the material starts to move towards the deeper end and this allows proper mixing of the material. Silica has a very high melting point, thus, to reduce its melting point soda ash is added. Lime stone is added, to make glass insoluble in water. As the mixture melts, a jelly like substance is formed and this jelly like substance forms glass on cooling. The manufactured glass is known as soda-lime glass. The time required for the formation of glass is nearly seven days.

1.3.2 *Toughened Glass*

The toughened glass has far more resistance to breakage compared to simple annealed glass, and also if it breaks, it will break in a more predictable way. Toughened glass is made by treating annealed glass with a thermal tempering process. A sheet of annealed glass is heated above 600° C *i.e.*, above its annealing point, its surfaces is rapidly cooled leaving the inner core hot. The different cooling rates between the surface and the inside of the glass produce different physical properties; resulting in compressive stresses on the surface and tensile stress in the core of the glass. This tensile stress balances the compressive stress at the surface of the glass. These opposite stresses give toughened glass resistance to breakage and even if it breaks, it breaks into small square pieces which are less dangerous than that of the larger pieces. Toughened glass also has an increased resistance to breakage as a result of stresses caused by different temperatures within a pane. It is five times stronger than that of the annealed glass. The tempering process improves the following properties:

- Thermal Stress
- Thermal Shock
- Tensile Strength

The following properties remained unchanged during tempering:

- Colour
- Clarity
- Chemical Composition
- Light Transmission
- Thermal Conductivity

1.3.3 *Laminated Glass*

Laminated glass consists of two or more layers of glass and a plastic film is sandwiched between the two layers of glasses. Depending upon the sandwiched plastic layer, the laminated glass is produced in two ways:

- **Poly-Vinyl Butyral (PVB) laminated glass:** In poly-vinyl butyral laminated glass, a layer of poly-vinyl butyral is sandwiched between the two glasses by means of pressure and heat. Other polymers such as Polyurethane (PU) or Ethyl Vinyl Acetate (EVA) can also be used.
- **Cast in Place (CIP) laminated glass:** Cast in Place (CIP) laminated glass is made by pouring resin in the space between two sheets of glass which are held parallel and very close to each other.

Laminated glass has many advantages such as security and safety. So, during impact the laminated glass breaks, but does not get shattered into the pieces. The broken pieces are held together by the layer of poly-vinyl butyral. This reduces the safety hazard linked with the shattered glass fragments, as well as the security risks associated with easy penetration. The interlayer also provides an easy way to apply several other techniques such as colouring, sound proofing, resistance-to-fire, ultra-violet filtering and other technologies that can be embedded within the interlayer. Laminated glass is widely used in buildings and automobiles. In building, it is used as a window glass and in automobiles it is used as a windshield.

1.4 Windshield

Earlier windshields or windscreen were made of ordinary glasses, but were not appropriate from the safety point of view as it could lead to serious injuries when any accident happens. So, these glasses were replaced with windshields which were made of toughened glass and are fitted in the frame using some type of sealant such as rubber or neoprene seal. The drawback of the toughened glass is that it breaks very easily even from a simple stone chip. It gets shattered into many harmless pieces when it breaks. In 1919, the owner of Ford named Henry Ford solved the problem of windshield by using the French technology called as laminated glass.

The windshields are made up of two layers of glasses and an inner layer is sandwiched between the two layers of glasses. This inner layer holds the glass together when it gets fractured. From the year 1919, Ford ordered the use of laminated glass on all of his company vehicles. Windshields protect the occupants from dirt, wind and flying debris such as insects, dust, smoke of vehicles and rocks. It also provides an aerodynamically shape at the front of vehicle. UV coating may be applied to screen to restrict harmful ultra-violet radiation. But it is unnecessary because almost all auto windshields are made up of laminated safety glass. The majority of UV-B is absorbed by the glass itself, and any remaining UV-B together with most of the UV-A is absorbed by the PVB bonding layer.

Fig. 1.1 Windshield of a car

1.5 Side Glass

Side glasses of an automobile are generally made up of tempered glass. The tempered glass has a property of not breaking into the sharp edges. Thus, it provides safety to the vehicle occupant if any accident occurs. The toughened glass is made by treating annealed glass with a thermal tempering process. A sheet of annealed glass is heated above 600° C *i.e.*, above its annealing point, then its surfaces is rapidly cooled leaving the inner core hot. The different cooling rates between the surface and the core of the glass produce different physical properties, resulting in compressive stresses on the surface which is balanced by tensile stresses produced in the core of the glass.

Fig. 1.2 Side glass of a car

1.6 Modes of Heat Transfer

The heat transfer or the mode of heat transfer is brought in lime light because the rise in temperature in the interior of the car cabin is due to the solar radiation entering into the interior of the car cabin.

The modes of heat transfer are

- **Conduction:** It is the energy transfer at a system boundary due to a temperature difference. The mechanism used for the heat transfer is inter-molecular interactions and this mechanism needs matter. The conduction equation was given by Fourier and is known as Fourier's law and is given by

$$Q = -KA\frac{dt}{dx} \tag{1.1}$$

where, Q = Heat transfer per unit area, K = Thermal conductivity of material, A = Cross sectional area and $\frac{dt}{dx}$ = Temperature gradient.

- **Convection:** It is the energy transfer across a system boundary due to a temperature difference by the combined mechanism of bulk transport and inter-molecular interactions. It needs fluid matter for heat transfer to take place.

  Newton's law of cooling:

$$Q = hA\Delta t \tag{1.2}$$

  where Q = Heat transfer per unit area, h = Convective heat transfer coefficient, A = Surface area and Δt = Temperature difference between surface and the fluid

- **Radiation:** Heat transfer with radiation takes place in the form of electromagnetic waves. It does not require any material medium for moving from one point to another. The energy is carried by electromagnetic waves in the form of small packets and does not involve the movement or the interaction of matter. The thermal radiation does not require any material medium and it can pass through matter as well as in vacuum. In fact, the heat energy received by the earth from the sun is in the form of electromagnetic waves. All objects above absolute zero degree temperature radiate energy in the form of electromagnetic waves. The rate of energy released by any object is directly proportional to the fourth power of absolute temperature. The Emissive power of a surface is given as

$$E = \sigma\varepsilon T_s^4 \tag{1.3}$$

  where E= Emissive power of a body, σ = Stefan Boltzmann constant, ε = Emissivity and T_s = Temperature.

The hotter the object, more it radiates the electromagnetic waves. Temperature also affects the wavelength and frequency of the radiated waves. Objects at room temperatures radiate infrared waves. Being invisible to the human eye, people cannot see infrared radiation. The energy radiated by an object is usually a collection of wavelengths. This is

usually referred to as an emission spectrum. As the temperature increases, the wavelengths of the radiation emitted by an object decreases. Hotter objects emit radiation of smaller wavelength, higher frequency and vice versa.

1.7 Contribution of Thesis

The contribution of the thesis is as follows:

- To develop a cabin which is made up of toughened glass and a wooden frame. The wooden frame will act as the supporting structure.
- To perform experiments on enclosed volume having the same phenomenon, as that of heat getting accumulated in car cabin due to solar radiation.
- To perform experiment on single layer toughened glass cabin for heat accumulation.
- To measure the temperature and heat flux in the cabin.
- To prepare a Bond Graph model of single layer glass cabin.
- To perform experiment on a box, which is made up of two layers of toughened glass and air is trapped in between the two glasses.
- To prepare a Bond Graph model of double layer toughened glass with air in between the two glasses.
- To perform experiment on a box, which is made up of two layers of toughened glass and argon is trapped in between the two glasses.
- To prepare a Bond Graph model of double layer toughened glass with argon trapped in between the two glasses.
- To perform experiment on a box, which is made up of two layers of toughened glass and argon is flowing in between the two glasses.
- To prepare a Bond Graph model of double layer toughened glass with argon flowing in between the two glasses.
- To compare the temperatures in the interior of the box experimentally and by simulation.

1.8 Organization of Thesis

Five chapters are included in this Thesis. Overview of the information included in the various chapters is as follows:

First chapter includes the introduction part, type of glasses, role of the wind shield, side glass, rear glass, materials of these glasses and the heat treatment process applied on the glass.

Literature review related to different modelling techniques for vehicle thermal comfort is included in the second chapter. Various developments in the automobiles to enhance the thermal comfort are given in the literature. Literature gap and objective of this thesis are also included in this chapter.

Basic principles of Bond Graph and its applications in modelling of thermal systems are given the third chapter. This chapter also includes the basics of Bond Graph modelling and thermal Bond Graph model for vehicle thermal comfort. Simulation results for temperature development in the compartment are also presented.

Fourth chapter includes the experimental setup. Experimental setup consists of closed box of toughened glass which is equivalent to a car compartment, two thermocouple, argon gas, two digital thermometers. Comparison between the simulation and experimental results is also included in this chapter.

Conclusion and scope for future work in presented in the fifth chapter.

CHAPTER 2 LITERATURE REVIEW

2.1 Introduction

In this chapter, the literature review on vehicle thermal comfort, Bond Graph modelling, Bond Graph modelling of vehicle thermal comfort has been presented. This chapter consist of literature review on heat reduction in a closed system, restricting the heat to enter into the house, vehicle thermal comfort and the Bond Graph modelling for the heat reduction. In this closed system or the house, various strategies implemented for the reduction of heat has been illustrated in this chapter.

2.2 Cooling Energy Efficiency and Solar Radiation Effect on a System

Windows are the link between the external ambient and the internal room condition of a house [**1**]. In cold climate there is a heat loss of about 10–25% from the interior of the house toward the external atmosphere via windows. In hot climate the window is one of the source of solar heat entry and thus increasing the cooling load of the refrigeration system. Thus a double layer glass and an infrared absorbing gas is used to restrict the heat. Three different mixtures of gasses are used; a strongly absorbing gas, an intermediate absorbing gas and a gas transparent to the infrared radiation is used. Also a phase change material is used. It is concluded that the double layer glass window with absorbing gas in it is much more efficient than that of the phase change material.

A window assembly is designed and fabricated which comprise of dielectric/metal/dielectric (D/M/D) [**2**]. This is used on the glass surface. The metal use is silver and the refractive index calculated by the numerical calculation is in the range of 1.6–2.4. This layer of dielectric/metal/dielectric is deposited on the glass surface. The combination of dielectric used along with the silver as a metal is TiO_2/Ag/ TiO_2 or WO_3/Ag/ WO_3 or ZrO_2/Ag/ ZrO_2. After testing it was found that the windows with any of these coating of dielectrics performed well and their efficiency are nearly the same. This glazing gives visible light transmission of about 80%, Ultraviolet and solar infrared radiations are blocked above 90%, and thermal radiations suppressed by an amount of 95%. The temperature difference of about 8^0C is observed when one glass is coated with the dielectric and another glass is uncoated.

A coating is developed for the window glasses called as vanadium dioxide (VO_2). It is a nanocrystal structure [**3**]. The film of vanadium dioxide is infrared optically transparent

in the semiconductor phase at low temperature and highly reflective at high temperature. This multilayer structure is transparent to the visible light weather the temperature is high or low and is opaque for infrared light at high temperature.

A new solar-heat-reflective and hydrophilic coating is developed. This coating is deposited on glass substrates by radio-frequency sputtering method [**4**]. It is a multilayer film which consists of silicon dioxide (SiO_2), titanium dioxide (TiO_2) and a heat-resistant silver alloy. The purpose of this coating was to improve the spectral transmittance as well as spectral reflection property. The silver alloy deposited on the glass substrates forms an anatase layer at elevated temperature. The glass reflects most of the infrared light and transmits most of the visible light. The titanium dioxide (TiO_2) layer is used to increase the hydrophilicity. Thus this coating is bifunctional, it reflect most of the unwanted solar radiation and also auto cleans by using sunlight and the rain water.

Reflective glasses are developed, which are prepared by coating the glasses with a nanostructured titanium dioxide (TiO_2) and silicon dioxide (SiO_2) film using a dip coating technique [**5**]. These glasses have a visible transmittance greater than 70%, solar reflectance of about 30% and have a very high ultraviolet blockage. Due to such properties these monolithic windows have a wide application in architectural and automotive area. The glass substrate prepared by sol-dip process has a high visible light transmittance and good solar blockage.

Temperature distribution as well as the air-flow field distribution is analysed inside the passenger's compartment of automobile using commercial software FLUENT [**6**]. Using FLUENT 3-D the temperature distributions and air flow field is modelled in an automobile compartment with or without passengers. Further, the results obtained by the FLUENT are also validated with the data obtained from the experiment. The experiments were performed on the (Buick 1.8L), which is manufacture by Chevrolet.

It deals with the temperature control in the interior of a stationary automobile compartment which is directly facing the solar energy from the sun [**7**]. A thin layer of phase change material is placed at the ceiling of the automobile. This phase change material is placed in small packets. It absorbs all the heat coming from the sun towards the ceiling of the automobile and gets converted into the liquid form. Thus the temperature inside the car is at comfortable condition. The amount of PCM required so as to keep the interior of the automobile cool is about 755 g. The PCM is classified as organic and inorganic materials.

Paraffin is widely used as a phase change material as its melting point range, falls into the thermal comfort zone of human beings.

The diver suit used by the divers consist of the air as the insulation material, now instead of the air, argon was used as the insulation material as it has low thermal conductivity compared to the air [**8**]. Six divers were selected for the experiment having an average age of 26 years. Both air and argon gas were filled in the diver suit but the divers did not know which gas is filled in which suit. It was seen that there is not much difference in temperature with the use of argon and air, maybe it was due to the shivering energy generated by the divers while diving.

Mathematical study was done on two layer window along with solar control film [**9**]. The double pane window consists of the two vertical glasses, glass 1 is facing the interior of the room and the glass 2 is facing the external environment and the solar heat. A solar control film (SCF) is applied to the glass 1 for the cold climate and another solar control film (SCF) is applied to the glass 2 for the hot climate. Varying the separation distance between the glass, the heat flow and the solar radiation incident is analysed. Three cases were studied, Case-1: double pane window with solar control film, Case-2: double pane window only, Case-3: single layer glass. In order to reduce or increase the heat gain, the optimum distance between the two glasses should be more than 6 cm. The use of solar control film along with the double pane window reduces the heat flow from inside to outside up to 52%.

The thermal behaviour inside the compartment of the car was studied depending upon the climatic condition and the type of the material used for the manufacturing of the car [**10**]. The numerical study was done by means of nodal study and the finite difference method. The compartment was divided into two division solid node and the fluid node. The solid node consists of the materials of the compartment and the fluid node consists of the air inside the compartment. Effects of car colour, types of glazing, solar radiation from the sun, and radiative property of material were investigated. The main purpose is to reduce the power consumption of the air conditioning. It is done by reducing the solar radiation that penetrates the interior of the car.

Transmittance of the solar radiation through the glazed window is reduced by using two glass panes and connecting them in such a way that no air space is present between the two glass panes [**11**].

Experiment is performed by parking a salon car in direct sunlight and in un-shaded area [**12**]. The experiment is performed in six different stages depending upon the number of open windows of the car. The temperature at 12 different locations were measured and this value is used in 3-D simulation software FLUENT. The experiment and the simulation software revealed that most of the heat is accumulated at top of the dashboard and most of the heat is entering through windshield and the dashboard. The drop down of the window by some extent will reduce the temperature in the compartment as air starts flowing through the external environment.

Both theoretical and experimental study was conducted on thermal comfort inside an automobile [**13**]. To investigate the thermal comfort during the heating period, air velocity, temperature, humidity were measured at different locations inside the compartment of the automobile. The human body was divided into 16 parts and the effect of temperature on the parts were studied both experimental and theoretically. The results obtained from both experimental and theoretically model were same.

Simulated results are presented [**14**]. Simulation results with a variety of conditions reveal that: (1) a good choice for decreasing the cooling load in the summer time is increasing the inlet air temperature, not reducing the volume flow rate of the inlet air; (2) the thermal comfort in a compartment with given conditions depends on the number of persons in it. For the compartment studied, there were are two passengers in the compartment both of them were seated on the back seat; (3) the outside temperature has appreciable effect on the cooling load; (4) to decrease the cooling load one can change the material of the window (reducing its transmissivity) and improve thermal insulation on the vehicle body; (5) a better flow circulation near the compartment bottom is favourable to improve the uniformity of temperature field around the driver's foot zone. The inlet air direction should be kept horizontal.

This work is conducted because of two reasons, first was to investigate the serious threat to life of pets or children left in stationary car on a hot summers day and second one is to determine the time of death of homicide and suicide victims inside the car parked in direct sunlight with all of it doors and windows closed [**15**]. This paper demonstrates that when a vehicle is parked in the sun, temperature level in the vehicle rises to temperature which is 20^0C more than that of the ambient temperature. A simple 'greenhouse' model was developed, for predicting the daily internal vehicle temperatures using readily available local meteorological data. This statistical model was calibrated using meteorological data and

temperature data collected on parked vehicles over several summer seasons. The model uses environmental temperature and radiation data as input, and is shown to predict cabin temperatures within about 1^0C. Both the data collected and the model developed show that the temperature inside the cabin of a black vehicle is typically 5^0C higher than that inside a white vehicle on a hot summer day. Also lowering the driver's side window of the vehicle by 2.5 cm, reduces cabin temperatures by 3^0C, which is not sufficient to reduce significantly the safety concerns for children or pets left in parked vehicles.

The study deals with the effect of the solar radiation over the air flow and the temperature distribution in the compartment of the car [**16**]. For this purpose, transmittance and reflectance of various glasses were measured to determine the spectral characteristics of windshield by using a spectrophotometer. Using the measurement data, CFD simulations were performed for three cases by using the commercial CFD software (ANSYS Fluent 13.0) based on the D.O method *i.e.*, discrete ordinates method for solving radiative energy transfer equation. It was found that about 99% of solar energy intensity was in the wavelength range of 280 nm and 2500 nm on the basis of the standard solar spectrum (ASTM G173). In particular, strong deflection of air flows were observed near the front seat and it could generate higher mixing region due to the complex vertical flows. The predicted temperature rise in the compartment of the car is approximately 3^0C resulting from spectral variation of transmittance and reflectance. Therefore, the spectral solar radiation effect should be considered while modelling thermal and the air flow field.

The study deals with the thermal modelling of the car cabin and controls the temperature by means of the fuzzy logic controller [**17**]. Thus ventilation and thermal loads were estimated first and then the equations of energy conservation and dry air mass of the cabin were derived and solved simultaneously. The data obtained from the thermal modelling of a car cabin was compared with the experimental hot room test. To maintain the thermal comfort of a cabin and controlling the blower outgoing air velocity and the circulated air percentage, a fuzzy controller was applied. Results showed that using a fuzzy controller, the time taken to control the compartment temperature is less and the time spent for cooling and ventilating the cabin was less and also the fuel consumption was reduced.

It provides a comprehensive review of the different models developed to predict vehicular cabins thermal comfort, in addition to the different experimental techniques used [**18**]. The review classifies the in-cabin modeling into; human physiological and psychological perspectives in addition to the compartment zone and the human thermal

manikin modelling. The experimental approaches are mainly the subjective observers, the thermal manikins, and the Infrared Thermo-graphy. Additionally the manuscript discusses and analyses each of the thermal indices that are typically used in assessing the in cabin conditions such as the Predicted Mean Value PMV index and the Predicted Percentage Dissatisfied PPD. The text also highlights the main attributes of vehicular thermal comfort, in terms of its fast transient behaviour, the in-homogeneity in the thermal fields associated with the high localized air velocity, solar loads and flux, in addition to the inherent variations related to the trip durations.

2.3 Heat Flow Analysis using Bond Graph

Bond Graph is a powerful tool for representing the systems which are from different domains such as thermal model of electronic system [**19**]. The Bond Graph library is created for modelling with the graphical Dymola support. It gives an idea of the basic tools of the Bond Graph for the new users. Bond Graph is very much suitable for the system that operates in a multi energy domain.

A new thermo Bond Graph library is developed for the modelling of the convective heat flow [**20**]. The process to use the new library has been demonstrated by an example-pressure cooker. The simulation of convective heat flow is done and it is not as difficult as creating a regular Bond Graph and also it is much more flexible to use.

Thermal behaviour of a building structure was determined [**21**]. The Bond Graph is use to model the heat transfer *i.e.*, conduction, convection and radiation from external environment to inside of the building. Bond Graph is very much suitable for modelling of heat transfer phenomenon specially conduction. The Dymola is used to convert the description provided into a readable code. The results are compared with CALPAS 3 and DOE-2 and it is found that the results are very much similar. Thus the Dymola is proved to be an excellent modelling tool.

It deals with the difficult problem of modelling of mass flowing in an thermodynamic system, *i.e.*, formulation with the mathematics of convective heat flow [**22**]. No quasi-stationary or flow-equilibrium assumption were made, such that the model generated using the proposed methodology would be as general as possible. The elements help the modeller to generate a simple thermodynamic system for the conduction and the convection heat transfer.

2.4 Literature Gap

After doing detailed study of literature on vehicle thermal comfort, it was observed that lot of research was done on the roof materials and air conditioning system in automobile. Also work has been done on windshield to enhance the thermal comfort by doing some type of coating on the glass or by using controllers. As per our knowledge very few works have been done on the reduction of the temperature inside the parked car compartment by using windshield and side glasses as double layer glass and filling a suitable gas in the separation layer of these glasses. So our research work will be on the toughened glasses which are used in automobile and the main aim of the research will be to reduce the heat getting accumulated into the car cabin parked in sunlight.

2.5 Objective of Work

According to the literature survey it is found that the double glass window will be helpful to obtain thermal comfort in the passenger compartment. The objective of present work is formulated and summary of these objectives are:

- To develop a physical model which is made up of toughened glass.
- To determine the gases having heat insulating properties.
- To conduct experiments on a box having single layer of toughened glass.
- To conduct experiments on a box having double layer of toughened glass and air in between the two glasses.
- To conduct experiments on a box having double layer of toughened glass and a gas which is an insulating gas flowing in between the two glasses.
- To conduct experiments on a box having double layer of toughened glass and a gas which is an insulating gas trapped in between the two glasses.
- To prepare a physical model of the system using Bond Graph theory.
- To verify the results obtained from physical model and the Bond Graph model.

CHAPTER 3 MODELLING THE COOLING EFFECT OF A SYSTEM QUIVALENT TO A CAR

3.1 Introduction

The dynamical equations of the system are obtained by the Hamilton's method and by the Lagrangian Method. These equations are solved so as to obtain the differential equation. If the equations are linear, they can be solved analytically but if the equations are nonlinear, there exist no analytical solution. Differential equations are obtained and are further solved with the help of computer. Obtaining and solving these differential equations manually can take more time. So, there was a need to develop solving technique which would not only automatically develop the differential equations but also solve the differential equations in a short period of time. This could be done by Bond Graph modelling technique. Bond Graph automatically generates the differential equation by modelling the system. In this chapter, Bond Graph is used to develop the thermal model of a closed system made up of multi layers of glasses. The temperature variations inside the closed system are modelled due to different heat intensities.

3.2 Bond Graph Modelling

In 1959, Prof. H. M. Paynter of MIT came up with an idea to develop the model of the system by means of the basic elements. This idea was portrayed in the form of symbolic representation know as Bond Graph. In Bond Graph, some essential information in the form of basic elements is to be conveyed and it is to be conveyed in such a manner that after conveying, the computer should perform a predefined algorithmic procedure to derive the differential equation. Some common basic elements for electrical or mechanical systems are inductor, resistor, capacitor, mass, spring, damper *etc*. Knowing what process is happening in the system and determining the basic elements required for the system, one can develop the system by putting all the basic elements in its proper position.

These elements interact with each other by means of energy or power. There is transfer of power between each element of the system. Transfer of power indirectly means transfer of effort and the flow as power is comprised of effort and the flow. Thus, there is actual transfer of the effort information and the flow information in different directions. The flow variable and the effort variable for different system are shown in Table 3.1.

Table 3.1: Power variables in different energy domains [**23**]

Systems	**Efforts (e)**	**Flow (f)**
Mechanical	Force (N)	Velocity ($m \cdot s^{-1}$)
	Torque (N-m)	Angular velocity ($rad \cdot s^{-1}$)
Electrical	Voltage (V)	Current (A)
Thermal	Temperature (K)	Entropy change rate ($W \cdot K^{1}$)
	Pressure ($N \cdot m^{-2}$)	Volume change rate ($m^3.s^{-1}$)
Hydraulic	Pressure ($N \cdot m^{-2}$)	Volume Flow rate ($m^3.s^{-1}$)
Chemical	Chemical potential ($N \cdot m \cdot mol^{-1}$)	Mass flow rate ($mol \cdot s^{-1}$)
	Entropy (Q/K)	Mass flow rate (kg/s)
Magnetic	Magnetic-motive force (An)	Magnetic flux rate ($Wb \cdot s^{-1}$)

3.2.1 *Bond Graph Standard Element*

The basic elements used in Bond Graph are represented as I, C, R, SE and SF. These basic elements are connected to each other by means of a line segment called bond. These bonds carry the power with them *i.e.,*, flow information and the effort information.

Bond Graph model can be divided into following four groups:

- Single port passive elements *i.e.,*, inertia (I), capacitance (C) and resistance (R).
- Active source elements *i.e.,*, source of effort (SE) and source of flow (SF).
- Two port conversion elements *i.e.,*, gyrator (GY) and transformer (TF).
- Junction elements *i.e.,*, flow summing junction (0) and effort summing junction (1)

3.2.2 *Basic 1-Port Element*

Single port element consists of single power port and at each single port it consists of a single pair of effort and flow variable. There are two types of ports *i.e.*,, passive port and the active port.

The inertia can also be called as inductor, compliance as capacitor, and resistor as dashpot. These are the passive elements because they are not power sources.

- **Compliance Element:** The compliant element is represented by a character 'C' with a bond ahead of it. This bond will be further connected to rest of the system. The bond carries the effort and the flow information. Such a device stores and gives up energy without loss example spring in mechanical system and capacitor in the electrical system. The graphical representation of compliant element is shown below.

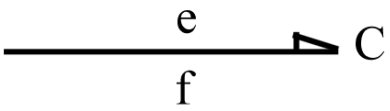

Fig. 3.1 Bond Graph representation of compliance element

In spring the effort (e) and the deformation (Q) is given as:

$$Q = \int_{-\infty}^{t} f \cdot dt \tag{3.1}$$

$$e = K \int_{-\infty}^{t} f \cdot dt \tag{3.2}$$

In capacitor, charge accumulated (Q) and voltage (e) is given as:

$$Q = \int_{-\infty}^{t} i \cdot dt \tag{3.3}$$

$$e = C^{-1} \int_{-\infty}^{t} i \cdot dt \tag{3.4}$$

In general compliant element is defined as

Effort= (constant or a function) $\times \int_{-\infty}^{now} flow \cdot dt$

- **Resistive Element:** Resistive element is an element in which the flow and the effort variables are related by a static function. It receives energy and dissipates it into the surrounding. The resistive element is represented by a character 'R' with a bond

ahead of it. The bond carries both effort and the flow information. The graphical representation of resistive element is shown below.

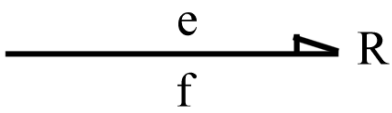

Fig. 3.2 Bond Graph representation of resistive element

The arrow is pointing toward the resistive element(R), which means that the power, which is the product of effort and the flow is positive and is flowing towards the resistive element.

In general resistive element is defined as

Effort = (a constant or a function) × (Flow),

Flow= (a constant or a function) × (Effort).

- **Inertial element:** This element gives the relationship between the effort and flow in such a way that integration of effort gives the flow. For example, mass in mechanical system and inductor in electrical system acts as inertial elements. The graphical representation of inertial element is shown below.

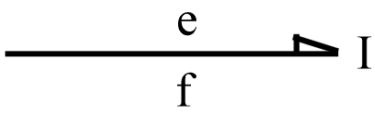

Fig. 3.3 Bond Graph representation of inertial element

The basic characteristic of inertial element is as follows:

For electrical system:

$$V = L\frac{di}{dt} \tag{3.5}$$

$$i(t) = \frac{1}{L}\int_{-\infty}^{t} V dt \tag{3.6}$$

For mechanical system: Force = rate of change of momentum

$$e = \frac{dP}{dt} \tag{3.7}$$

$$P(t) = \int_{-\infty}^{t} e dt \tag{3.8}$$

So, it can be written in general form:

Flow = (a constant or a function) $\times \int_{-\infty}^{t} (\text{effort}) dt$

- **Source of Effort:** The source of effort is represented by 'SE' with a bond ahead of it. It can independently decide the effort variable on the bond but it cannot decide the flow variable, the flow variable is decided by the rest of the system. The graphical representation is shown below.

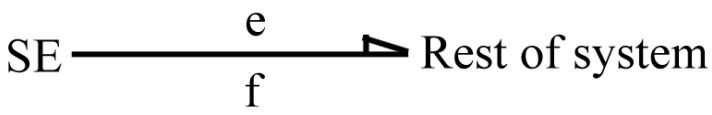

Fig. 3.4 Bond Graph representation of source of effort element

- **Source of Flow:** The character of flow element is that it can determine the flow information but it cannot decide the effort information, the effort information is decided by the rest of the system. The example of mechanical source of flow is cam. By rotating the cam it gives up and down motion to the piston.

Fig. 3.5 Bond Graph representation of source of flow element

3.2.3 *Basic 2-Port Element*

The basic 2-port elements are "Transformer" and the "Gyrator". The transformer is represented in Bond Graph as "TF" and the gyrator is represented as "GY". Both Transformer and the gyrator consist of two bonds on either side of it. The bond contains both flow and the effort information.

- **Transformer:** Transformer does not create nor it destroys energy, it only amplifies the energy. It conserves the power it receives and then it transmits the power with a certain scaling factor. It consists of two bonds on either side. Both the bond consists of effort and the flow information. For transformer the flow on one side is equal to the translational times the flow on the other side and the effort on one side is equal to the translational times the effort on the other side.

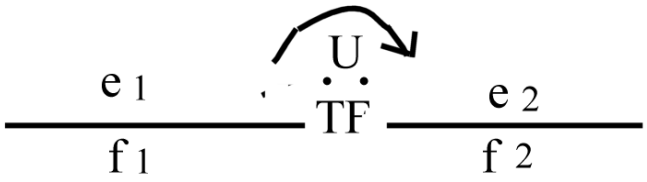

Fig. 3.6 Bond Graph representation of transformer element

$$f_2 = \mu \cdot f_1 \tag{3.9}$$

$$e_1 \cdot f_1 = e_2 \cdot f_2 \tag{3.10}$$

$$\therefore e_2 = \frac{1}{\mu} e_1 \tag{3.11}$$

- **Gyrator:** Transformer provides a relation between flow to flow and the effort to effort but the gyrator provides a relation between flow to effort and vice versa keeping the power same on both the port. In gyrators there is no need to show arrows.

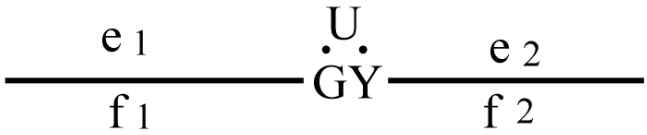

Fig. 3.7 Bond Graph representation of gyrator element

$$e_2 = \mu \cdot f_1 \tag{3.12}$$

$$e_1 \cdot f_1 = e_2 \cdot f_2 \tag{3.13}$$

$$e_1 = \mu \cdot f_2 \tag{3.14}$$

3.2.4 *Junctions*

In Bond Graph there are two types of junctions, 1-Junction and 0-Junction. The details of the junction are described below:

- **0-Junction:** 0-Junction has a property of equalizing the effort *i.e.*,, all the bonds connected to the 0-Junction will have same effort but different flow. Thus it is also called flow summing junction. The graphical representation of 0-Junction is given below

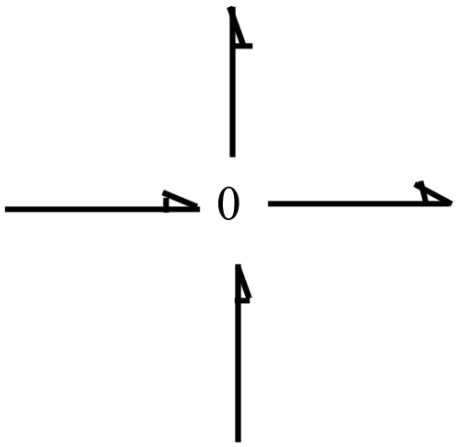

Fig. 3.8 Bond Graph representation of 0-junction

- **1-Junction:** 1-junction has a property of equalizing the flow in all bonds connected to it *i.e.*,, the flow is same in all bonds but the effort is different. The effort will be decided by the rest of the system. It is also called as the effort summing junction.

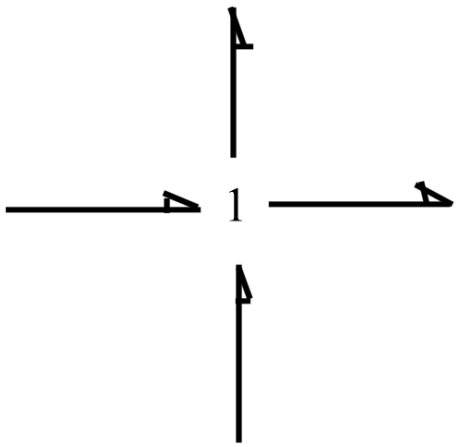

Fig. 3.9 Bond Graph representation of 1-junction

Table 3.2: Bond Graph element [**24**]

Type	Name	Symbol	Definition	
			Linear	Nonlinear
Storages	Inertia		$f = \frac{1}{m}\int_{-\infty}^{t} e\,\mathrm{d}t$	$f = \psi_{\mathrm{I}}\left(\int_{-\infty}^{t} e\,\mathrm{d}t\right)$
		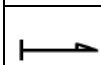	$e = m\frac{\mathrm{d}f}{\mathrm{d}t}$	$e = \phi_{\mathrm{I}}\left(\frac{\mathrm{d}f}{\mathrm{d}t}\right)$
	Capacitance		$e = K\int_{-\infty}^{t} f\,\mathrm{d}t$	$e = \phi_{\mathrm{C}}\left(\int_{-\infty}^{t} f\,\mathrm{d}t\right)$
		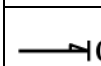	$f = \frac{1}{K}\frac{\mathrm{d}e}{\mathrm{d}t}$	$f = \psi_{\mathrm{C}}\left(\frac{\mathrm{d}e}{\mathrm{d}t}\right)$
Dissipation	Resistance		$f = e/R$	$f = \psi_{\mathrm{R}}(e)$
		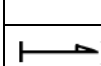	$e = R\,f$	$e = \phi_{\mathrm{R}}(f)$
Transducers (ideal)	Gyrator I	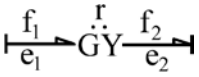	$e_2 = r\,f_1$ $e_1 = r\,f_2$	$e_2 = r(x)\,f_1$ $e_1 = r(x)\,f_2$
	Gyrator II	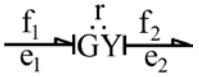	$f_1 = \frac{1}{r}e_2$ $f_2 = \frac{1}{r}e_1$	$f_1 = \frac{1}{r(x)}e_2$ $f_2 = \frac{1}{r(x)}e_1$
	Transformer I	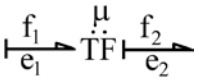	$f_2 = \mu\,f_1$ $e_1 = \mu\,e_2$	$f_2 = \mu(x)\,f_1$ $e_1 = \mu(x)\,e_2$
	Transformer II	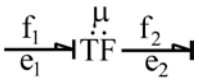	$f_1 = \frac{1}{\mu}f_2$ $e_2 = \frac{1}{\mu}e_1$	$f_1 = \frac{1}{\mu(x)}f_2$ $e_2 = \frac{1}{\mu(x)}e_1$
Sources	Source of	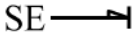	$e = e(t)$	

	effort		
	Source of flow	SF	$f = f(t)$
Junctions	Zero (0)	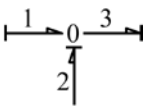	$e_1 = e_2 = e_3$ $f_1 + f_2 = f_3$
	One (1)	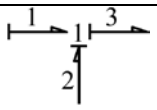	$f_1 = f_2 = f_3$ $e_1 + e_2 = e_3$

3.2.5 *Causality*

Causality means establishing a relation between the cause and the effect of the cause. It is shown by a small vertical stroke at the start or at the end. This causality indicates the effort and the flow direction. Both the effort and the flow direction is always opposite to each other.

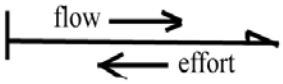

(a)

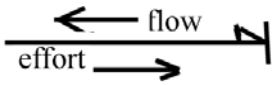

(b)

Fig. 3.10 Causality concept

As shown in Fig. 3.10 the small vertical line helps in determining the effort and the flow direction. If the flow is going toward the half arrow then the causality symbol (vertical line) is give at the back of the line as shown in Fig. 3.10(a). For this condition the effort will be always opposite to the flow so it will in the direction as shown in Fig. 3.10(a). The same rule is applicable for the Fig. 3.10(b). The elaborated discussion on Bond Graph element is given below:

- **Causality of Source of Effort (Se):** It determines the effort information but cannot determine the flow information. It provides the effort information to the rest of the system and their on the rest of the system provides the flow information to the Se element. The graphical representation of causality of source of effort is shown in the

Fig. 3.11. The ‘Se’ element provides effort information to rest of the system and the rest of system provides the flow information to ‘Se’ element. The vertical bar at the end of the bond indicates the direction of flow. The direction of flow is from vertical bar toward the ‘Se’ element.

Fig. 3.11 Causality of source of effort

- **Causality of Source of Flow (Sf):** The source of flow determines the flow information and provides this information to the rest of the system. The rest of the system provides effort information to ‘Sf’ element. The graphical representation is shown in the Fig. 3.12.

Fig. 3.12 Causality of source of flow

- **Causality of Inertial Element (I):** Inertial element takes the effort information from rest of the system and gives flow information to the rest of the system. For inertial element, integrated effort gives the flow information. Thus effort is the cause and the result of this cause is flow, which is the effect. The graphical representation is shown in the Fig. 3.13.

Fig. 3.13 Integral causality of inertial element

- **Causality of Compliance Element (C):** Capacitive element stores energy and give it whenever required without any energy loss. For Compliant element, flow is required so that effort can happen. It means flow is the cause and effort is the effect of that cause. The general equation of causality of compliance element and the graphical representation is shown below:

Fig. 3.14 Integral causality of compliant element

- **Causality of Resistive Element (R):** The resistive element does not have time integral form of constitutive law. There is a direct relation between the flow and the effort variable. Thus flow can be cause and the effort can be effect of the cause or effort can be cause and the flow can be effect of that cause.

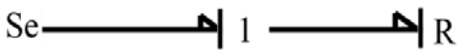

Fig. 3.15 Causality of resistive element

- **Causality of Transformer Element (TF):** The transformer element receives flow information in one bond and the same information is further transferred to the next bond. The causality of transformer element can be shown in two forms.

(a)

(b)

Fig. 3.16 Causality of tranformer element, (a) when flow is from left to right. (b) when flow is from right to left.

- **Causality of Gyrator Element:** Gyrator element relates effort to flow or the flow to effort. Thus both of its port is either open-ended or stroke-ended causality. The causality of gyrator element is as follows.

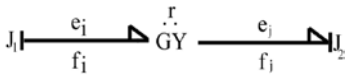

(a)

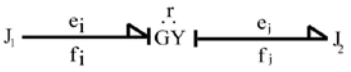

(b)

Fig. 3.17 Causality of gyrator element

- **Causality of Junction Element:** 0-Junction is the effort equalising junction *i.e.*,, the effort in all the bonds connected to 0-Junction is equal. For example four bonds are connected to 0-Junction, then the flow information can be brought in by any number of bonds say three in this case and effort information can be brought in by only one bond and this effort information is equally distributed in all the bonds connected to 0-Junction.

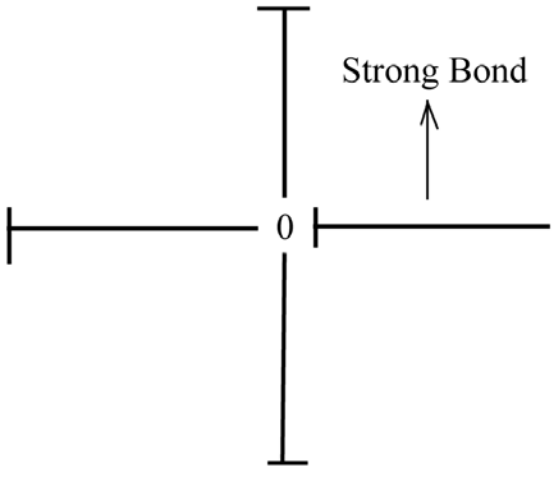

Fig. 3.18 Causality of 0-junction

Similarly in 1-junction, only one bond can bring in the flow information and rest of the bond will bring in the effort information. The flow information brought in by the bond is equally distributed to bonds connected to the 1-junction.

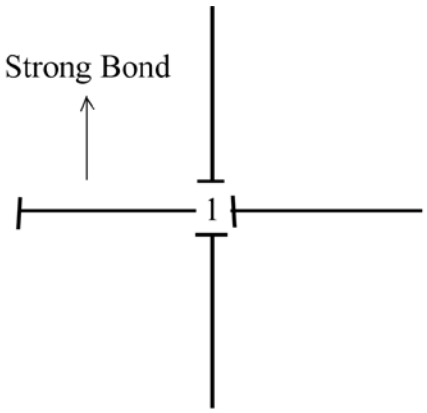

Fig. 3.19 Causality of 1-junction

3.3 Thermal Modelling of the System Surrounded by a Single Layer of Glass

Toughened glass having a dimension 548 mm × 310 mm × 5 mm is fitted into the wooden frame (Fig. 3.20). Wooden frame is acting as a supporting structure for the glass. This assembly of wooden frame and the glass is equivalent to the internal compartment of a car. The glass is properly sealed with sealant so that no air can escape from the assembly. Clay is used as a sealant for glass and frame. The frame is insulated with thermocol from top and the bottom so that no heat could escape. The entire setup is exposed to the direct solar heat waves. This single glass model is further modeled with the help of Bond Graph so that the results can be validated experimentally as well as theoretically. The Bond Graph model for single layer is given in Fig. 3.21.

Fig. 3.20 Cabin made up of single glass layer

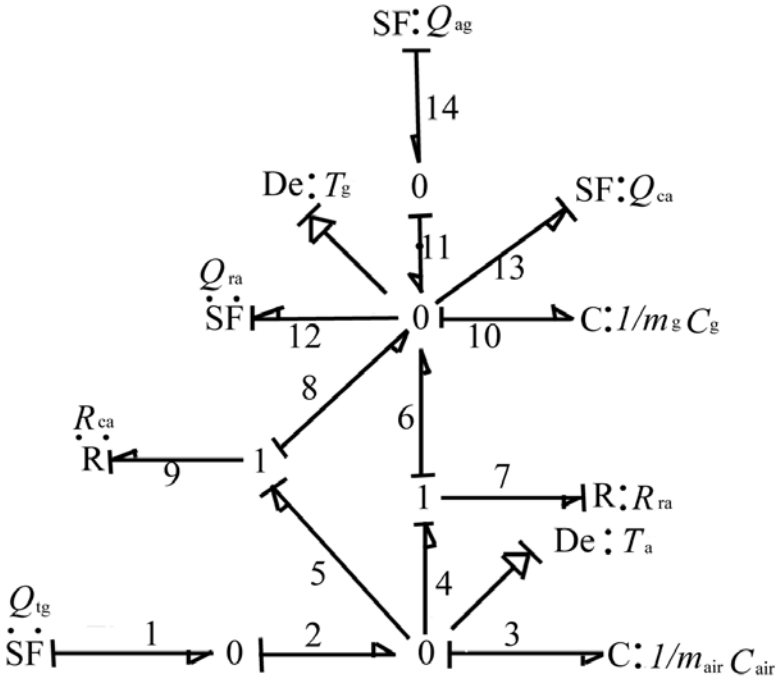

Fig. 3.21 Bond Graph model of single glass layer

From the total heat flux coming to the glass surface, the heat will be absorbed, reflected and transmitted. As shown in the Fig. 3.21 above SF14 represents the amount of heat absorbed by the glass surface (Q_{ag}) which is given by.

$$Q_{ag} = I_r \times A \times a_g \tag{3.15}$$

where I_r=Irradiance, A=Area, a_g= Absorptivity of glass.

At this point of time the glass has been heated to a high temperature and the glass has itself becomes a heating source and starts to radiate the heat from its surface into the surrounding. Q_{ra} represents the amount of heat radiated (SF12) by the glass surface into the surroundings.

$$Q_{ra} = e_g \times \sigma \times A \times ((T_{ga})^4 - (T_{sa})^4) \tag{3.16}$$

where Q_{ra}= Radiative heat transfer, e_g= Emissivity of glass, σ= Stefan Boltzmann Constant, T_{ga}= Glass temperature, T_{sa}= Space Temperature.

Some of the heat from the glass surface will be taken away by the surrounding air by convection. As shown in Fig. 3.21 Q_{ca} is the heat flow (SF13) by convection into the surrounding.

$$Q_{ca} = h_{ca} \times A \times (T_{ga} - T_{a1}) \tag{3.17}$$

where Q_{ca}= Convective heat transfer, h_{ca}= Convective heat transfer coefficient of outside air, A= Area, T_{ga}= Glass Temperature, T_{a1}= Atmospheric temperature.

The R_{ca} (R9) is convective thermal resistance, for the heat flowing from inside air to the surface of the glass. It offers resistance to the heat flow. The equation of the convective thermal resistance is obtained by comparing it with the general heat transfer equation.

$$Q_{conv} = A \times h_{air} \times \Delta T \tag{3.18}$$

General heat transfer equation,

$$Q = \frac{\Delta T}{R_{th}} \tag{3.19}$$

Comparing Eq. (3.18) and Eq. (3.19), the value of convective thermal resistance (R_{th}) is given by

$$R_{th} = R_{ca} = \frac{1}{A \times h_{air}} \tag{3.20}$$

where R_{ca}= Convective thermal resistance, A= Area of glass, h_{air}= Convective heat transfer coefficient of air.

Similarly, R_{ra} is radiative thermal resistance (R7) for the radiative heat flow from inside air to the surface of the glass. The radiative thermal resistance can be obtained as follows:

$$\begin{aligned}
Q_{rad} &= A \times e_{air} \times \sigma \times (T_{aa}{}^4 - T_{ga}{}^4) \\
Q_{rad} &= A \times e_{air} \times \sigma \times ((T_{aa}{}^2)^2 - (T_{ga}{}^2)^2) \\
Q_{rad} &= A \times e_{air} \times \sigma \times (T_{aa}{}^2 + T_{ga}{}^2) \times (T_{aa}{}^2 - T_{ga}{}^2) \\
Q_{rad} &= A \times e_{air} \times \sigma \times (T_{aa}{}^2 + T_{ga}{}^2) \times (T_{aa} + T_{ga}) \times (T_{aa} - T_{ga}) \\
\therefore T_{aa} - T_{ga} &= \frac{Q_{rad}}{A \times e_{air} \times \sigma \times (T_{aa}{}^2 + T_{ga}{}^2) \times (T_{aa} + T_{ga})}
\end{aligned} \tag{3.21}$$

Comparing Eq. (3.21) with general Eq. (3.19), the value of R_{th} is given by

$$R_{th} = R_{ra} = \frac{1}{A \times e_{air} \times \sigma \times (T_{aa}{}^2 + T_{ga}{}^2) \times (T_{aa} + T_{ga})} \tag{3.22}$$

where R_{ra}= Radiative thermal resistance, σ= Stefan Boltzmann Constant, T_{aa}= Inside air temperature, T_{ga}= Glass temperature.

C10 is the compliance element, it takes the flow *i.e.*,, heat absorbed by the glass and gives the effort information *i.e.*,, the temperature of the glass. This temperature of the glass can be detected by the effort detector (De) connected at the 0-junction.

$$K10 = \frac{1}{m_g \times C_g} \tag{3.23}$$

where $K10$= Compliance element, m_g= Mass of glass, C_g= Specific heat of glass.

Now from the total heat received, a part of the heat will be absorbed, reflected and transmitted. The SF1 bond represents the heat transmitted by the glass and this heat will be absorbed by the inside air. Thus, the total amount of heat transmitted by the glass is given by

$$Q_{tg} = I_r \times A \times t_g \tag{3.24}$$

where Q_{tg}= Heat transmitted by the glass, I_r= Irradiance, A=Area, t_g=Transmissivity of glass.

The compliant element C3 will give the effort information *i.e.*,, the temperature of the air inside the glass compartment. A detector (De) is connected at 0-junction which will give the value of rise of temperature of air inside the glass compartment.

$$K3 = \frac{1}{m_{air} \times C_{air}} \tag{3.25}$$

where $K3$= Compliance element, m_g= Mass of glass, C_g= Specific heat of glass.

3.3.1 *Parameter Values*

The parameter values for the simulation are given Table 3.3.

Table 3.3: Parameter values for single layer glass cabin

Parameter	Value	Description
A	0.68 m^2	Area
h_{air}	8 W/m^2-K	Convective heat transfer coefficient of air
e_{air}	0.01	Emissivity of air
σ	5.67x10^{-8}	Stefan Boltzmann Constant
m_{air}	0.063 kg	Mass of air
C_{air}	919 kJ/kg-K	Specific heat of air
m_g	23.4 kg	Mass of glass
C_g	720 kJ/kg-K	Specific heat of glass
T_s	-261^{0}C	Temperature of space
e_g	0.9	Emissivity of glass
I_r	110 W/m^2	Heat flux
a_g	0.25	Absorptivity of glass
t_g	0.5	Transmissivity of glass

h_{ca}	10 W/m^{2}K	Convective heat transfer coefficient

3.3.2 *Simulation Results*

The different parameters obtained by doing practical experiments, were used as the input to Bond Graph model of single layer glass. The various parameters used as the input for the single glass Bond Graph model was, atmospheric temperature, heat flux, various properties of toughened glasses and the air. The result obtained by the Bond Graph model of the single glass layer is show in Fig. 3.22.

Table 3.4: Simulation results of single layer glass cabin

Sl. No.	T (Hour)	ST (^{0}C)	SRCCT (^{0}C)	SRGT (^{0}C)	Y (W/m^2)
1	0	38	38	38	110
2	0.25	38	50.3	43.5	
3	0.5	39	54.66	47.9	
4	1	38.1	56.6	49.78	
5	1.5	38.2	57.48	50.66	
6	2	38.9	58.6	51.8	
7	2.5	39.1	59.4	52.58	

where T= Time, ST= Surrounding Temperature, SRCCT= Simulation Results Central Cabin Temperature and SRGT= Simulation Results Glass Temperature.

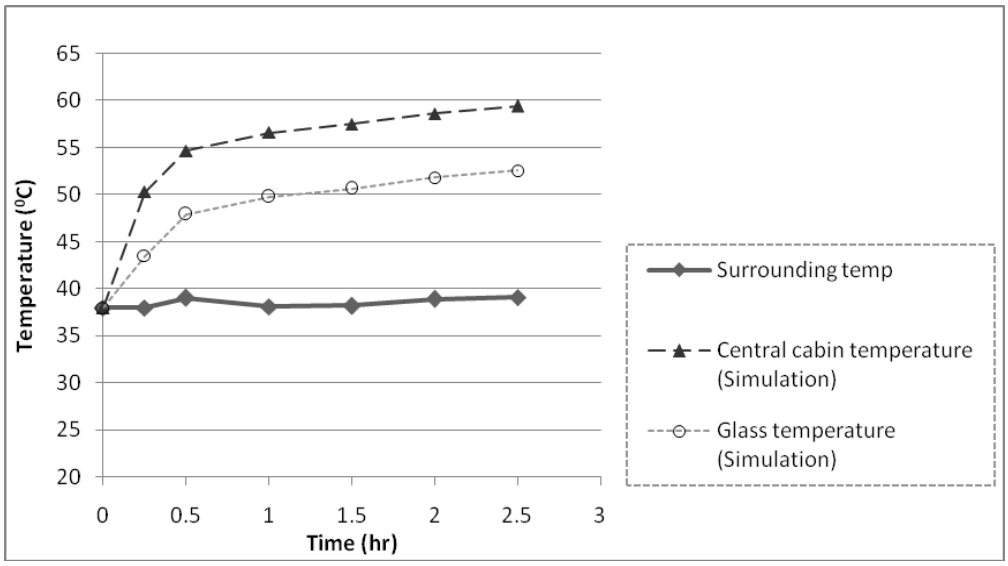

Fig. 3.22 Simulation results of single layer glass

3.4 Thermal Modelling of the System Surrounded by Double Layer of Glass with Air between Two Glasses

In this phase of the experiment two toughened glasses having dimension of 548 mm × 310 mm × 5 mm are used. These two glasses are assembled together in such a way that there is a gap of 10 mm in between the two glasses. For this purpose, a separator is used which is having a thickness of 10 mm, this separator is made up of wood and has a dimension 20 mm × 20 mm × 10 mm. Four pieces of such separator are placed at each corner of the glass and the other glass is placed over it so as to form an assembly. Further, this double glass is sealed with a tape so that it becomes a single unit. In the similar fashion three more such assemblies are made which would be further fitted into the wooden frame and a cabin will be prepared. This entire setup is placed in an open environment *i.e.*,, in direct solar light. Due to the solar heat wave, the temperature in the interior of the cabin will go on increasing. This results obtained by the experiment will be used as the input for the Bond Graph model shown in Fig. 3.23 below. The entire system explained above will be modeled in the Bond Graph so that the validation can be done between the simulation results and the experimental results.

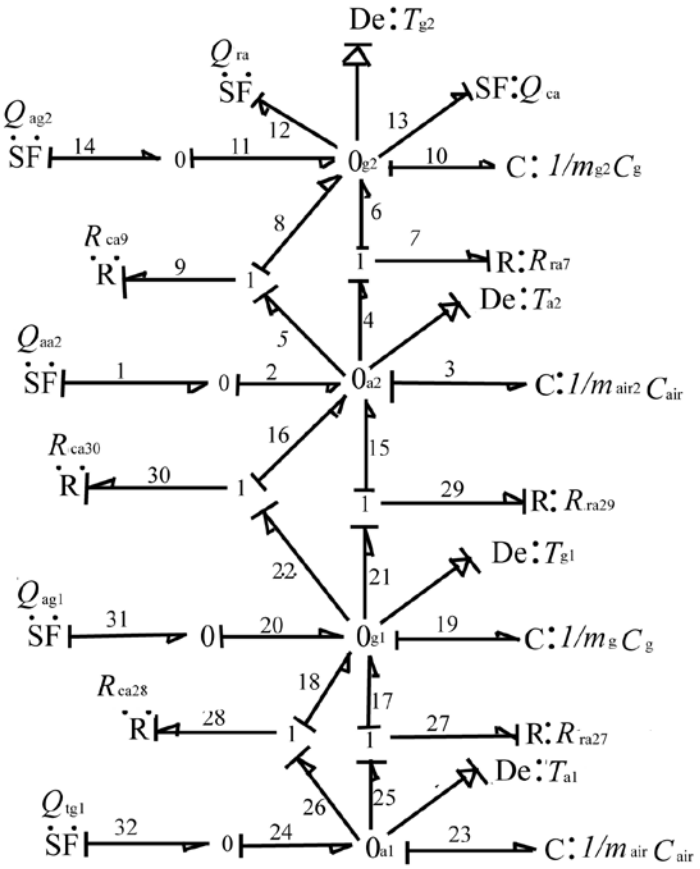

Fig. 3.23 Bond Graph of double glass layer with air trapped condition

As shown in Fig. 3.23, the outer glass is in direct contact with the environment. Sunlight directly falls on the outer glass. Some part of the heat flux falling on the outer glass will be absorbed by the glass, some part will be reflected back and some part will be transmitted through the outer glass. The heat absorbed (SF14) by the outer glass is represented by Q_{ag2}. As there are two layers of glasses separated by an air gap of 10 mm, this trapped air will absorb some part of the heat transmitted by the outer glass. The remaining transmitted heat after getting absorbed by the air gap will be reflected by the inner glass. From this reflected heat, again a part of the heat will be absorbed by the air present in between the two glasses. The rest of the reflected heat after getting absorbed by the air in between the two glasses will be further absorbed by the outer glass. So, the total heat absorbed by the outer glass is

$$Q_{ag2} = I_r \times A \times a_g + I_r \times A \times t_g \times (1 - a_a) \times r_g \times (1 - a_a) \times a_g \tag{3.26}$$

where Q_{ag2}= Heat absorbed by outer glass, I_r= Solar heat flux, A= Area of glass, a_g= Absorptivity of glass, t_g= Transmissivity of glass, a_a= Absorptivity of air, r_g= Reflectivity of glass.

Now, the outer glass will get heated and will itself become a heat source. The heat will be radiated by the outer glass into the atmosphere and thus there will be a loss of the heat from the glass. There will also be heat loss by convection from the outer glass to the surrounding. The heat radiated and convected by the outer glass to the surrounding is given as

$$Q_{ra} = e_g \times \sigma \times A \times ((T_{ga})^4 - (T_{sa})^4) \tag{3.27}$$

where Q_{ra}= Heat radiated by outer glass, e_g= Emissivity of glass, A= Area of glass, T_{ga}= Outer glass temperature, T_{sa}= Space temperature and

$$Q_{ca} = h_{ca} \times A \times (T_{ga} - T_{a1}) \tag{3.28}$$

where Q_{ca}= Heat transfer by convection from outer glass, h_{ca}= Convective heat transfer coefficient of glass, A= Area of glass, T_{ga}= Outer glass Temperature, T_{a1}= Atmospheric temperature.

As shown C10 is the compliance element. It takes in the flow information and gives the effort information. In this case the flow is the heat flux (Q) absorbed by the outer glass, this heat flow rate is integrated and further multiplied by a factor which gives the effort *i.e.*,, the temperature of the outer glass. An effort detector (De) is connected to 0_{g2}-junction as shown in the Fig. 3.23. This detector gives the temperature of the outer glass.

$$K10 = \frac{1}{m_{g2} \times C_g} \tag{3.29}$$

where K10= Capacitive element, m_{g2}= Mass of outer glass, C_g= Specific heat of glass.

R_{ca9} and the R_{ra7} are convective and the radiative thermal resistance respectively between the outer glass and the air present in between the two glass layers. It offers a resistance to the heat flow between the outer glass and the air present in between the two glass layer. As shown, the effort from the 1-junction combines with the respective resistive element *i.e.*,, Convective thermal resistance and the resistive thermal resistance and gives back flow information which is heat flow (Q). This heat causes the change of the temperature of the outer glass and this change can be detected by means of the effort detector (De) connected at 0_{g2}-junction. The radiative and the convective thermal resistance are given as

$$R_{ra7} = \frac{1}{A \times e_{air} \times \sigma \times ((T_{aa2})^2 + (T_{ga2})^2) \times (T_{aa2} + T_{ga2})} \tag{3.30}$$

where R_{ra7}= Radiative thermal resistance, A= Area of glass, e_{air}= Emissivity of air in between the two glass, σ= Stefan Boltzmann Constant, T_{ga2}= Temperature at outer glass (0_{g2}), T_{aa2}= Temperature of atmospheric air present in between two glass (0_{a2}) and

$$R_{ca9} = \frac{1}{A \times h_{air}} \tag{3.31}$$

where R_{ca9}= Convective thermal resistance, A= Area of glass, h_{air}= Convective heat transfer coefficient of air.

Now, the outer glass has received some heat flux from the sun, out of this heat some heat will be transmitted by the outer glass. Some part of this transmitted heat will be absorbed by the air present in between the two glasses; the remaining unabsorbed heat will be further reflected by the inner glass. From the total reflected heat, again some of the heat will be absorbed by the air in between the two glasses. The total amount of heat absorbed by the air in between the two glasses is represented by Q_{aa2} as shown in the Fig. 3.23. The total heat absorbed by the air will be

$$Q_{aa2} = I_r \times A \times t_g \times a_a + I_r \times A \times t_g \times (1 - a_a) \times r_g \times a_a \tag{3.32}$$

where Q_{aa2}= Heat absorbed by the air present in between two glass, I_r= Solar heat flux, A= Area of glass, t_g= Transmissivity of glass, a_a= Absorptivity of air, r_g= Reflectivity of glass.

The compliance element C3 will take as an input the amount of heat absorbed by the air present between the two glass layers and gives the rise in temperature of the air. This temperature rise of the air is further detected by the effort detector (De) connected to 0_{a2}-junction as shown in Fig. 3.23.

$$K3 = \frac{1}{m_{air2} \times C_{air}} \tag{3.33}$$

where $K3$= Capacitive element, m_{air2}= Mass of air present in between two glass, C_{air}= Specific heat of air.

R_{ca30} and the R_{ra29} are convective and the radiative thermal resistance respectively between the air present between the two glass layer and the inner glass. It offers a resistance to the heat flow between the air present between the two glass layer and the inner glass. The convective and the radiative thermal resistance is given as

$$R_{\text{ca30}} = \frac{1}{A \times h_{\text{air}}} \tag{3.34}$$

where R_{ca30}= Convective thermal resistance, A= Area of glass, h_{air}= Convective heat transfer coefficient of air and

$$R_{\text{ra29}} = \frac{1}{A \times e_{\text{air}} \times \sigma \times ((T_{\text{a11}})^2 + (T_{\text{ga1}})^2) \times (T_{\text{a11}} + T_{\text{ga1}})} \tag{3.35}$$

where, R_{ra29}= Radiative thermal resistance, A= Area of glass, e_{air}= Emissivity of air in between the two glass, σ= Stefan Boltzmann Constant, T_{ga1}= Temperature of inner glass, T_{a11}= Temperature of atmospheric air present in between two glass.

As shown in Fig. 3.23, Q_{ag1} is the amount of heat absorbed by the inner glass. From the total heat transmitted by the outer glass, some part of the transmitted heat is absorbed by the air in between the two glass, remaining heat is further transmitted towards the inner glass. From the heat received by the inner glass a part of the heat will be absorbed by the inner glass. This absorption of the heat increases the temperature of the inner glass. The capacitive element C19 will take in the flow (Q) and give effort information of the inner glass *i.e.*,, temperature of the inner glass. This temperature of the inner glass can be detected by the effort detector (De) connected to 0_{g1}-junction. The heat absorbed by the inner glass and the compliant element C19 is given as

$$Q_{\text{ag1}} = I_{\text{r}} \times A \times t_{\text{g}} \times (1 - a_{\text{a}}) \times a_{\text{g}} \tag{3.36}$$

where Q_{ag1}= Heat absorbed by the inner glass, I_{r}= Solar heat flux, A= Area of glass, t_{g}= Transmissivity of glass, a_{a}= Absorptivity of air, a_{g}= Absorptivity of glass.

$$K19 = \frac{1}{m_{\text{g}} \times C_{\text{g}}} \tag{3.37}$$

where K19= Capacitive element, m_{g}= Mass of glass, C_{g}= Specific heat of glass.

Again R_{ca28} and R_{ra27} is the convective and the resistive thermal resistance respectively between the inner glass and the air present inside the closed cabin made up of glass. It offers resistance to heat flow. These resistances are given by

$$R_{\text{ca28}} = \frac{1}{A \times h_{\text{air}}} \tag{3.38}$$

where R_{ca28}= Convective thermal resistance, A= Area of glass, h_{air}= Convective heat transfer coefficient of air and

$$R_{ra27} = \frac{1}{A \times e_{air} \times \sigma \times ((T_{aa})^2 + (T_{ga})^2) \times (T_{aa} + T_{ga})} \tag{3.39}$$

where R_{ra27}= Radiative thermal resistance, A= Area, e_{air}= Emissivity of air inside the glass cabin, σ= Stefan Boltzmann Constant, T_{ga}= Temperature of inner of the glass, T_{aa}= Temperature of atmospheric air present inside the glass cabin.

As shown in Fig. 3.23, out of the total heat transmitted by the outer glass , some of the heat will be absorbed by the air present in between the two glasses and also some of the heat will be absorbed by the inner glass. The remaining heat will be transmitted by the inner glass into the internal chamber of the closed cabin. This transmitted heat will continuously increase the temperature of the air present inside the closed chamber as this heat could not be escaped from the closed chamber. This transmitted heat is represented by Q_{tg1} as shown in the Fig. 3.23 above. The transmitted heat is given by

$$Q_{tg1} = I_r \times A \times t_g \times (1 - a_a) \times t_g \tag{3.40}$$

where Q_{tg1}= Heat transmitted by the inner glass, I_r= Solar heat flux, A= Area of glass, t_g= Transmissivity of glass, a_a= Absorptivity of air.

The C23 is the compliance element which takes the flow *i.e.*,, the heat flow and gives the effort *i.e.*,, the temperature. This temperature can be detected by the effort detector (De) connected to 0_{a1} junction in the Bond Graph shown above in Fig. 3.23

$$K23 = \frac{1}{m_{air} \times C_{air}} \tag{3.41}$$

where K23= Capacitive element, m_{air}= Mass of air inside the cabin, C_{air}= Specific heat of air.

3.4.1 Parameter Values

Table 3.5: Parameter values for double layer glass cabin, air trapped condition

Parameter	Value	Description
A	0.68 m^2	Area
h_{air}	8 W/m^2-K	Convective heat transfer coefficient of inside air
e_{air}	0.01	Emissivity of air
σ	5.67x10^{-8}	Stefan Boltzmann Constant
m_{air}	0.063 kg	Mass of air
m_{air2}	0.00806288 kg	Mass of air present in between two glass
C_{air}	919 kJ/kg-K	Specific heat of air
m_{g1}	23.4 kg	Mass of outer glass
m_{g2}	23.4 kg	Mass of inner glass
C_g	720 kJ/kg-K	Specific heat of glass
T_s	-261^{0}C	Temperature of space
e_g	0.9	Emissivity of glass
I_r	118 W/m^2	Heat flux
a_a	0.01	Absorbtivity of air
a_g	0.25	Absorptivity of glass
t_g	0.5	Transmissivity of glass
r_g	0.25	Reflectivity of glass
h_{ca}	10 W/m^2K	Convective heat transfer coefficient of outer air

3.4.2 *Simulation Results*

The different parameters obtained by doing practical experiments were used as the input to Bond Graph model of double layer glass. The various parameters used as the input for the Bond Graph model were atmospheric temperature, heat flux, various properties of toughened glasses and the air. The result obtained by the Bond Graph model of the double glass layer with air in between the two glasses is show in Fig. 3.24.

Table 3.6: Simulation results of double layer glass cabin, air trapped condition

Sl. No.	T (Hour)	ST (^{0}C)	SRCCT (^{0}C)	SROGT (^{0}C)	SRIGT (^{0}C)	SRATT (^{0}C)	Y (W/m^2)
1	0	36.5	36.5	36.5	36.5	36.5	118
2	0.25	36.5	41.8	40	38.2	39.1	
3	0.5	37.3	44.5	42.9	40.9	41.9	
4	1	37.4	48.2	45.1	44.6	44.9	
5	1.5	38.1	52	47	48.4	47.7	
6	2	38	54.4	47.8	50.8	49.3	
7	2.5	38.8	57.3	49.3	53.7	51.6	

where T= Time, ST= Surrounding Temperature, SRCCT= Simulation Results Central Cabin Temperature, SROGT= Simulation Results Outer Glass Temperature, SRIGT= Simulation Results Inner Glass Temperature, Y= Solar Heat Flux, SRATT= Simulation Results Air Trapped Temperature.

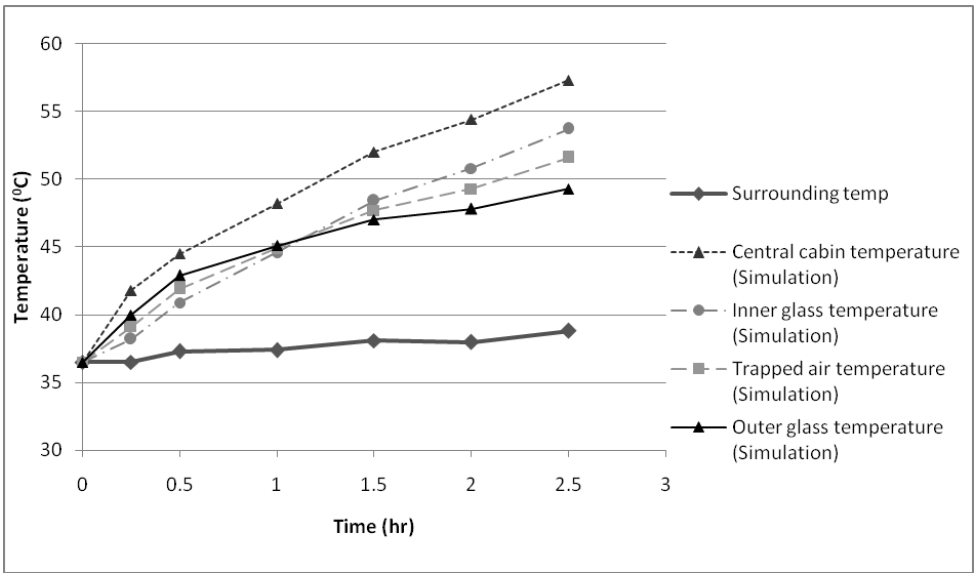

Fig. 3.24 Simulation results of double layer glass with trapped air

3.5 Thermal Modelling of a System Surrounded by Double Layer of Glass with Argon Between the Two Glasses

The experiments performed is similar to that of performed in the double glass with the air trapped in between the glasses, only the difference is that instead of the air, argon is used as the insulating gas. As the argon gas is having a low thermal conductivity it allows less heat to conduct through it. Also as the argon is trapped *i.e.,* no movement of the argon, there is no heat flow by convection. As explained in the air trapped condition, a separator is used in the argon trapped condition.

The entire setup is placed in direct solar light so that the heat can be accumulated into the glass box. Results obtained by the practical experiment will be used as the input for the Bond Graph model shown in Fig. 3.26. The entire system explained above will be modeled in the Bond Graph so that the validation can be done between the simulation results and the experimental results.

Fig. 3.25 Double layer glass cabin, argon trapped condtion

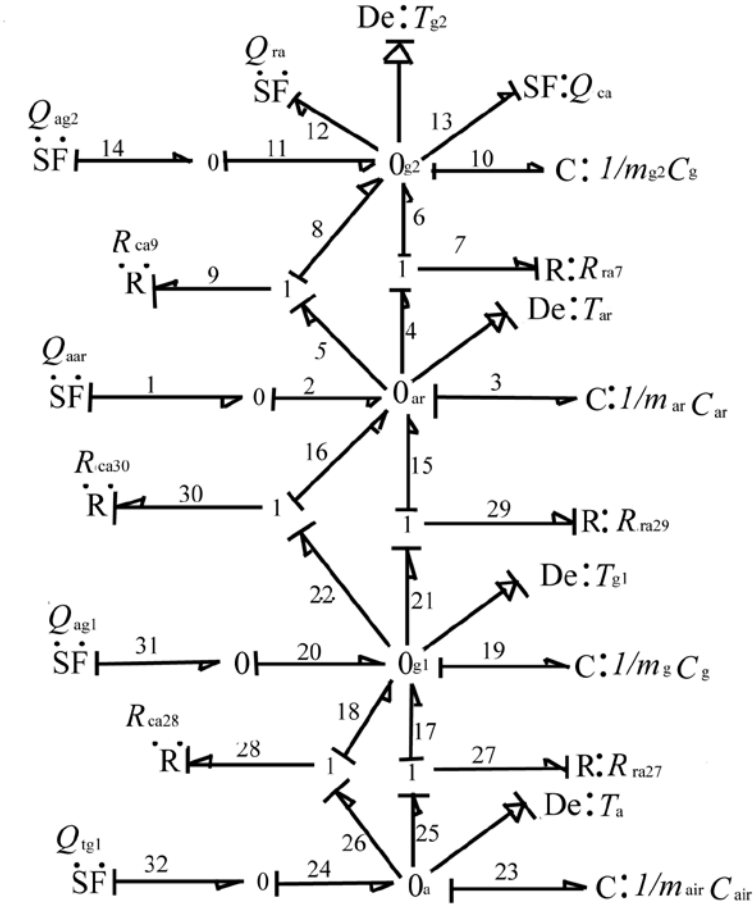

Fig. 3.26 Bond Graph of double layer glass with trapped argon

As shown in the Fig. 3.26, the outer glass is in direct contact with environment. Heat flux directly comes to the outer glass, some part of the heat, falling on the glass will be absorbed by the glass and some part will be transmitted through the outer glass. The heat absorbed by the outer glass is represented by Q_{ag2}. There are two layers of glasses which are separated by 10 mm; in this gap a gas called argon gas is trapped. This argon gas will absorb some part of the heat transmitted by the outer glass. The remaining transmitted heat after getting absorbed by the argon gas will be reflected by the inner glass. From this reflected heat, again a part of the heat will be again absorbed by the argon gas present in between the two glasses. The rest of the reflected heat from the inner glass will be further absorbed by the outer glass. So, the total heat absorbed by the outer glass is

$$Q_{ag2} = I_r \times A \times a_g + I_r \times A \times t_g \times (1 - a_{ar}) \times r_g \times (1 - a_{ar}) \times a_g \tag{3.42}$$

where $Q_{ag2=}$ Heat absorbed by outer glass, I_r= Solar heat flux, A= Area of glass, a_g= Absorptivity of glass, t_g= Transmissivity of glass, a_{ar}= Absorptivity of argon gas, r_g= Reflectivity of glass.

Now, the outer glass will get heated and will itself become a heat source. Heat will be radiated from the outer glass to the atmosphere and thus there will be a loss of the heat by radiation from the outer glass. There will also be heat loss by convection from the outer glass to the surroundings. The heat radiated and convected by the outer glass to the surrounding are given by

$$Q_{ra} = e_g \times \sigma \times A \times ((T_{ga})^4 - (T_{sa})^4) \tag{3.43}$$

where Q_{ra}= Heat radiated by outer glass, e_g= Emissivity of glass, A= Area of glass, T_{ga}= Outer glass temperature, T_{sa}= Space temperature and

$$Q_{ca} = h_{ca} \times A \times (T_{ga} - T_{a1}) \tag{3.44}$$

where Q_{ca}= Heat transfer by convection from outer glass, h_{ca}= Convective heat transfer coefficient of glass, A= Area of glass, T_{ga}= Outer glass Temperature, T_{a1}= Atmospheric temperature.

As shown C10 is the compliance element. It takes the flow information and gives the effort information. In this case the flow is the heat (Q) absorbed by the outer glass, this heat is further multiplied by a factor which gives the effort *i.e.,* the temperature of the outer glass.

An effort detector (De) is connected to 0_{g2}-junction as shown in the Fig. 3.26. This detector gives the temperature of the outer glass.

$$K10 = \frac{1}{m_{g2} \times C_g} \tag{3.45}$$

where $K10$= Capacitive element, m_{g2}= Mass of outer glass, C_g= Specific heat of glass.

R_{ca9} and the R_{ra7} are convective and the radiative thermal resistance, respectively between the outer glass and the argon gas present in between the two glass layer. It offers a resistance to the heat flow between the outer glass and the argon gas present in between the two glass layer. The resistive and the convective thermal resistance are given as

$$R_{ra7} = \frac{1}{A \times e_{ar} \times \sigma \times ((T_{aa2})^2 + (T_{ga2})^2) \times (T_{aa2} + T_{ga2})} \tag{3.46}$$

where R_{ra7}= Radiative thermal resistance, A= Area of glass, e_{air}= Emissivity of air in between the two glass, σ= Stefan Boltzmann Constant, T_{ga2}= Temperature of outer glass, T_{aa2}= Temperature of argon gas present in between two glass.

$$R_{ca9} = \frac{1}{A \times h_{ar}} \tag{3.47}$$

where R_{ca9}= Convective thermal resistance, A= Area of glass, h_{ar}= Convective heat transfer coefficient of argon gas.

Now, the outer glass has received some heat flux received from the sun, out of this heat some heat will be transmitted by the outer glass. Some part of this transmitted heat will be absorbed by the argon gas present in between the two glasses; the remaining unabsorbed heat will be further reflected by the inner glass. From the total reflected heat again some of the heat will be absorbed by the argon gas present in between the two glasses. The total amount of heat absorbed by the argon gas is represented by Q_{aar} as shown in Fig. 3.26. The total heat absorbed by the argon will be

$$Q_{aar} = I_r \times A \times t_g \times a_{ar} + I_r \times A \times t_g \times (1 - a_{ar}) \times r_g \times a_{ar} \tag{3.48}$$

where Q_{aar}= Heat absorbed by the argon gas present in between two glass, I_r= Solar heat flux, A= Area of glass, t_g= Transmissivity of glass, a_{ar}= Absorptivity of argon, r_g= Reflectivity of glass.

The compliance element C3 will take as an input, the amount of heat absorbed by the argon gas present between the two glass layers and gives rise in temperature of the argon.

This temperature rise of the argon is further detected by the effort detector (De) connected to 0_{ar}- junction as shown in Fig. 3.26

$$K3 = \frac{1}{m_{ar} \times C_{ar}} \tag{3.49}$$

where $K3$= Capacitive element, m_{ar}= Mass of argon present in between two glass, C_{ar}= Specific heat of argon.

R_{ca30} and the R_{ra29} are convective and the radiative thermal resistance respectively between the argon present between the two glass layer and the inner glass. It offers a resistance to the heat flow between the argon present between the two glass layer and the inner glass. The convective and the radiative thermal resistance is given as

$$R_{ca30} = \frac{1}{A \times h_{ar}} \tag{3.50}$$

where R_{ca30}= Convective thermal resistance, A= Area of glass, h_{ar}= Convective heat transfer coefficient of argon gas and

$$R_{ra29} = \frac{1}{A \times e_{ar} \times \sigma \times ((T_{a11})^2 + (T_{ga1})^2) \times (T_{a11} + T_{ga1})} \tag{3.51}$$

where R_{ra29}= Radiative thermal resistance, A= Area of glass, e_{ar}= Emissivity of argon gas, σ= Stefan Boltzmann Constant, T_{ga1}= Temperature of inner glass, T_{a11}= Temperature of argon gas.

As shown in Fig. 3.26, Q_{ag1} is the amount of heat absorbed by the inner glass. From the total heat transmitted by the outer glass, some part of the transmitted heat is absorbed by the argon; remaining heat is further transmitted towards the inner glass. From the heat received by the inner glass, a part of the heat will be absorbed by the inner glass. This absorption of the heat increases the temperature of the inner glass. The capacitive element C19 will take in the flow (Q) and give effort information of the inner glass *i.e.,* temperature of the inner glass. This temperature of the inner glass can be detected by the effort detector connected to inner glass (0_{g1}). The heat absorbed by the inner glass and the compliant element C19 is given as

$$Q_{ag1} = I_r \times A \times t_g \times (1 - a_{ar}) \times a_g \tag{3.52}$$

where Q_{ag1}= Heat absorbed by the inner glass, I_r= Solar heat flux, A= Area of glass, t_g= Transmissivity of glass, a_{ar}= Absorptivity of argon gas, a_g= Absorptivity of glass.

$$K19 = \frac{1}{m_g \times C_g} \tag{3.53}$$

where $K19$= Capacitive element, m_g= Mass of glass, C_g= Specific heat of glass.

Again, R_{ca28} and R_{ra27} are the convective and the resistive thermal resistance, respectively between the inner glass and the air present inside the closed cabin made up of glass. It offers resistance to heat flow. These resistances are given by

$$R_{ca28} = \frac{1}{A \times h_{air}} \tag{3.54}$$

where R_{ca28}= Convective thermal resistance, A= Area of glass, h_{air}= Convective heat transfer coefficient of air and

$$R_{ra27} = \frac{1}{A \times e_{air} \times \sigma \times ((T_{aa})^2 + (T_{ga})^2) \times (T_{aa} + T_{ga})} \tag{3.55}$$

where R_{ra27}= Radiative thermal resistance, A= Area, e_{air}= Emissivity of air inside the glass cabin, σ= Stefan Boltzmann Constant, T_{ga}= Temperature of inner glass, T_{aa}= Temperature of air present inside the glass cabin.

As shown in Fig. 3.26, out of the total heat transmitted by the outer glass, some of the heat will be absorbed by the argon gas and also some of the heat will be absorbed by the inner glass. The remaining heat will be transmitted through the inner glass into the internal chamber of the closed cabin. This transmitted heat will continuously increase the temperature of the air present inside the closed chamber as this heat could not be escaped from the closed chamber. This transmitted heat is represented by Q_{tg1} as shown in Fig. 3.26. The transmitted heat is given by

$$Q_{tg1} = I_r \times A \times t_g \times (1 - a_{ar}) \times t_g \tag{3.56}$$

where Q_{tg1}= Heat transmitted by the inner glass, I_r= Solar heat flux, A= Area of glass, t_g= Transmissivity of glass, a_{ar}= Absorptivity of argon gas.

The C23 is the compliance element which takes the flow *i.e.*,, the heat flow and gives the effort *i.e.*, the temperature. This temperature can be detected by the effort detector (De) connected to (0_a) junction in the Bond Graph shown above in Fig. 3.26

$$K23 = \frac{1}{m_{air} \times C_{air}} \tag{3.57}$$

where $K23$= Capacitive element, m_{air}= Mass of air inside the cabin, C_{air}= Specific heat of air.

3.5.1 *Parameter Values*

Table 3.7: Parameter values for double layer glass cabin, argon trapped condition

Parameter	Value	Description
A	0.68 m^2	Area of glass
h_{air}	8 W/m^2-K	Convective heat transfer coefficient of air
h_{ar}	5.3 W/m^2K	Convective heat transfer coefficient of argon gas
e_{ar}	0.05	Emissivity of argon gas
e_{air}	0.01	Emissivity of air
σ	5.67x10^{-8}	Stefan Boltzmann Constant
m_{ar}	0.01209546 kg	Mass of argon gas
m_{air}	0.063 kg	Mass of air
C_{ar}	520 kJ/kg-K	Specific heat of argon gas
C_{air}	919 kJ/kg-K	Specific heat of air
m_g	23.4 kg	Mass of outer glass
m_{g2}	23.4 kg	Mass of inner glass
C_g	720 kJ/kg-K	Specific heat of glass
T_s	-261^{0}C	Temperature of space
e_g	0.9	Emissivity of glass
I_r	100 W/m^2	Heat flux
a_{ar}	0.1	Absorbtivity of argon
a_g	0.25	Absorptivity of glass
t_g	0.5	Transmissivity of glass
r_g	0.25	Reflectivity of glass
h_{ca}	10.25 W/m^2K	Convective heat transfer coefficient of glass

3.5.2 *Simulation Results*

The different parameters obtained by doing practical experiments, were used as the input to Bond Graph model of double layer glass with argon gas trapped as shown in Fig. 3.26. The parameters used as the input for the Bond Graph model were, atmospheric temperature, heat flux, various properties of toughened glasses, air and argon. The result obtained by the Bond Graph model of the double glass layer with argon trapped is show in Fig. 3.27.

Table 3.8: Simulation results of double layer glass cabin, argon trapped condition

Sl. No.	T (Hour)	ST (^{0}C)	SRCCT (^{0}C)	SROGT (^{0}C)	SRIGT (^{0}C)	SRTAT (^{0}C)	Y (W/m^2)
1	0	36	36	36	36	36	100
2	0.25	36	40.25	39.34	37.47	38.68	
3	0.5	38	43.86	43.49	41.09	42.52	
4	1	39.1	48.18	47.11	45.41	46.56	
5	1.5	39.5	51.52	48.88	48.74	49.25	
6	2	39.4	53.95	49.52	51.17	50.95	
7	2.5	40.4	57.08	51.26	54.3	53.5	

Where T= Time, ST= Surrounding Temperature, SRCCT= Simulation Results Central Cabin Temperature, SROGT= Simulation Results Outer Glass Temperature, SRIGT= Simulation Results Inner Glass Temperature, Y= Solar Heat Flux, SRTAT= Simulation Results Trapped Argon Temperature.

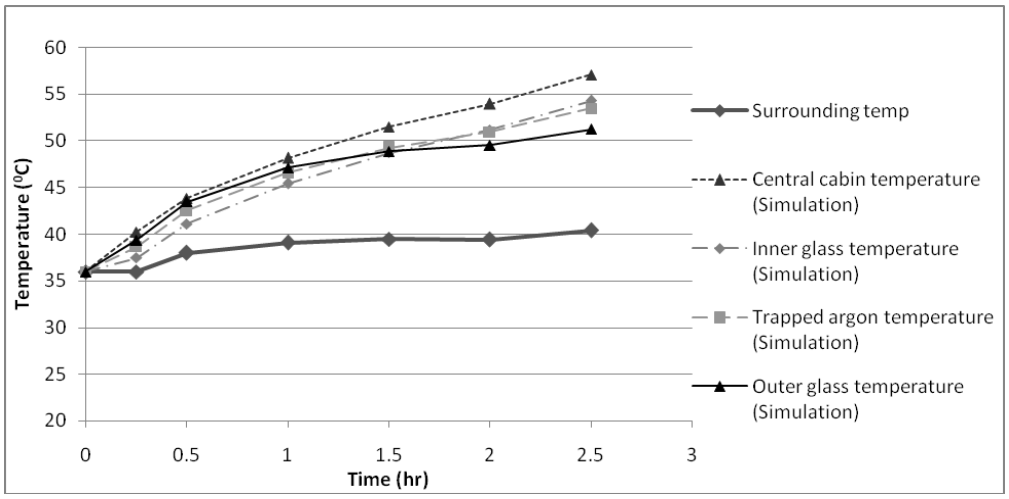

Fig. 3.27 Simulation results of double layer glass with trapped argon

3.6 Therma Modelling of the System Surrounded by Double Layer of Glass with Flowing Argon Between Two Glasses

Entire process is similar to the process explained for the double layer glass with argon gas trapped in it. Only the difference is that, the argon gas in this case is not trapped but it is contineously flowing through the system. The Bond Graph model for the double layer of glass with flowing argon between the two glasses is described in Fig. 3.28.

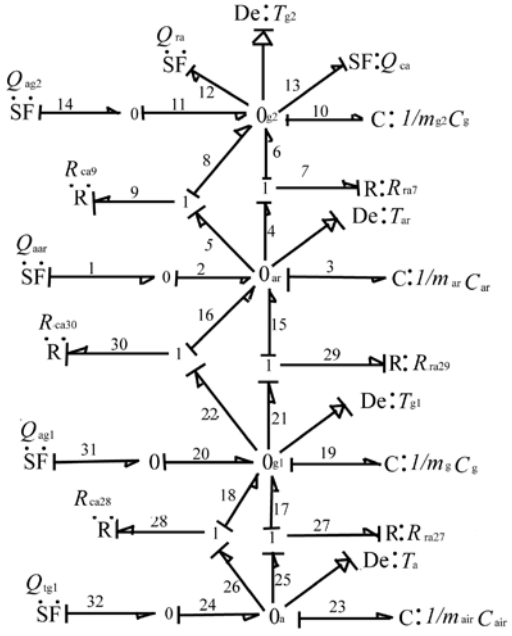

Fig. 3.28 Bond Graph of double layer glass with flowing argon

As shown in Fig. 3.28, the outer glass is in direct contact with environment. Heat directly falls on the outer glass; some part of the heat, falling on the glass will be absorbed by the glass and some part will be transmitted through the outer glass. The heat absorbed by the outer glass is represented by Q_{ag2}. There are two layers of glasses which are separated by 10 mm; in this gap a gas called argon gas is continuously flowing. This argon gas will absorb some part of the heat transmitted by the outer glass. The remaining transmitted heat after getting absorbed by the argon gas will be reflected by the inner glass. From this reflected heat, again a part of the heat will be again absorbed by the argon gas flowing in between the two glasses. The rest of the reflected heat from the inner glass will be further absorbed by the outer glass. So the total heat absorbed by the outer glass is

$$Q_{ag2} = I_r \times A \times a_g + I_r \times A \times t_g \times (1 - a_{ar}) \times r_g \times (1 - a_{ar}) \times a_g \tag{3.58}$$

where $Q_{ag2=}$ Heat absorbed by outer glass, I_r= Solar heat flux, A= Area of glass, a_g= Absorptivity of glass, t_g= Transmissivity of glass, a_{ar}= Absorptivity of argon gas, r_g= Reflectivity of glass.

Now, the outer glass will get heated and will itself become a heat source. Heat will be radiated from the outer glass to the atmosphere and thus there will be a loss of the heat by radiation from the outer glass. There will also be heat loss by convection from the outer glass to the surroundings. The heat radiated and convected by the outer glass to the surrounding are given by

$$Q_{ra} = e_g \times \sigma \times A \times ((T_{ga})^4 - (T_{sa})^4) \tag{3.59}$$

where Q_{ra}= Heat radiated by outer glass, e_g= Emissivity of glass, A= Area of glass, T_{ga}= Outer glass temperature, T_{sa}= Space temperature and

$$Q_{ca} = h_{ca} \times A \times (T_{ga} - T_{a1}) \tag{3.60}$$

where Q_{ca}= Heat transfer by convection from outer glass, h_{ca}= Convective heat transfer coefficient of glass, A= Area of glass, T_{ga}= Outer glass Temperature, T_{a1}= Atmospheric temperature.

As shown in Fig. 3.28, C10 is the compliance element. It takes in the flow information and gives the effort information. In this case the flow is the heat (Q) absorbed by the outer glass, this heat is further multiplied by a factor which gives the effort *i.e.,* the

temperature of the outer glass. An effort detector (De) is connected to 0_{g2}-junction as shown in Fig. 3.28. This detector gives the temperature of the outer glass.

$$K10 = \frac{1}{m_{g2} \times C_g} \tag{3.61}$$

where $K10$= Compliance, m_{g2}= Mass of outer glass, C_g= Specific heat of glass.

R_{ca9} and the R_{ra7} are convective and the radiative thermal resistance respectively between the outer glass and the argon gas flowing in between the two glass layer. It offers a resistance to the heat flow between the outer glass and the argon gas present in between the two glass layer. The resistive and the convective thermal resistance are given as

$$R_{ra7} = \frac{1}{A \times e_{air} \times \sigma \times ((T_{aa2})^2 + (T_{ga2})^2) \times (T_{aa2} + T_{ga2})} \tag{3.62}$$

where R_{ra7}= Radiative thermal resistance, A= Area of glass, e_{air}= Emissivity of air in between the two glass, σ= Stefan Boltzmann Constant, T_{ga2}= Temperature of outer glass, T_{aa2}= Temperature of argon gas present in between two glass.

$$R_{ca9} = \frac{1}{A \times h_{ar}} \tag{3.63}$$

where R_{ca9}= Convective thermal resistance, A= Area of glass, h_{ar}= Convective heat transfer coefficient of argon gas.

Now, the outer glass has received some heat flux received from the sun, out of this heat some heat will be transmitted by the outer glass. Some part of this transmitted heat will be absorbed by the argon gas flowing in between the two glasses; the remaining unabsorbed heat will be further reflected by the inner glass. From the total reflected heat again some of the heat will be absorbed by the argon gas present in between the two glasses. The total amount of heat absorbed by the argon gas is represented by Q_{aar} as shown in Fig. 3.28. The total heat absorbed by the argon will be

$$Q_{aar} = I_r \times A \times t_g \times a_{ar} + I_r \times A \times t_g \times (1 - a_{ar}) \times r_g \times a_{ar} \tag{3.64}$$

where Q_{aar}= Heat absorbed by the argon gas flowing in between two glass, I_r= Solar heat flux, A= Area of glass, t_g= Transmissivity of glass, a_{ar}= Absorptivity of argon, r_g= Reflectivity of glass.

The compliance element C3 will take as an input the amount of heat absorbed by the argon gas present between the two glass layers and gives rise in temperature of the argon.

This temperature rise of the argon is further detected by the effort detector (De) connected at junction 0_{ar} as shown in Fig. 3.28.

$$K3 = \frac{1}{m_{ar} \times C_{ar}} \tag{3.65}$$

where $K3$= Capacitive element, m_{ar}= Mass of argon present in between two glass, C_{ar}= Specific heat of argon.

R_{ca30} and the R_{ra29} are convective and the radiative thermal resistance respectively between the argon present between the two glass layer and the inner glass. It offers a resistance to the heat flow between the argon present between the two glass layer and the inner glass. The convective and the radiative thermal resistance is given as

$$R_{ca30} = \frac{1}{A \times h_{ar}} \tag{3.66}$$

where R_{ca30}= Convective thermal resistance, A= Area of glass, h_{ar}= Convective heat transfer coefficient of argon gas.

$$R_{ra29} = \frac{1}{A \times e_{ar} \times \sigma \times ((T_{a11})^2 + (T_{ga1})^2) \times (T_{a11} + T_{ga1})} \tag{3.67}$$

where R_{ra29}= Radiative thermal resistance, A= Area of glass, e_{ar}= Emissivity of argon gas, σ= Stefan Boltzmann Constant, T_{ga1}= Temperature of inner glass, T_{a11}= Temperature of argon gas.

As shown in Fig. 3.28, Q_{ag1} is the amount of heat absorbed by the inner glass. From the total heat transmitted by the outer glass, some part of the transmitted heat is absorbed by the argon; remaining heat is further transmitted towards the inner glass. From the heat received by the inner glass, a part of the heat will be absorbed by the inner glass. This absorption of the heat increases the temperature of the inner glass. The capacitive element C19 will take in the flow (Q) and give effort information of the inner glass *i.e.*, temperature of the inner glass. This temperature of the inner glass can be detected by the effort detector connected to 0_{g1}-junction. The heat absorbed by the inner glass and the compliant element C19 is given as

$$Q_{ag1} = I_r \times A \times t_g \times (1 - a_{ar}) \times a_g \tag{3.68}$$

where Q_{ag1}= Heat absorbed by the inner glass, I_r= Solar heat flux, A= Area of glass, t_g= Transmissivity of glass, a_{ar}= Absorptivity of argon gas, a_g= Absorptivity of glass and

$$K19 = \frac{1}{m_g \times C_g} \tag{3.69}$$

where $K19$= Capacitive element, m_g= Mass of glass, C_g= Specific heat of glass.

Again R_{ca28} and R_{ra27} is the convective and the resistive thermal resistance respectively between the inner glass and the air present inside the closed cabin made up of glass. It offers resistance to heat flow. These resistances are given by

$$R_{ca28} = \frac{1}{A \times h_{air}} \tag{3.70}$$

where R_{ca28}= Convective thermal resistance, A= Area of glass, h_{air}= Convective heat transfer coefficient of air.

$$R_{ra27} = \frac{1}{A \times e_{air} \times \sigma \times ((T_{aa})^2 + (T_{ga})^2) \times (T_{aa} + T_{ga})} \tag{3.71}$$

where R_{ra27}= Radiative thermal resistance, A= Area, e_{air}= Emissivity of air inside the glass cabin, σ= Stefan Boltzmann Constant, T_{ga}= Temperature of inner glass, T_{aa}= Temperature of air present inside the glass cabin.

As shown in Fig. 3.28, out of the total heat transmitted by the outer glass, some of the heat will be absorbed by the argon gas and also some of the heat will be absorbed by the inner glass. The remaining heat will be transmitted through the inner glass into the internal chamber of the closed cabin. This transmitted heat will continuously increase the temperature of the air present inside the closed chamber as this heat could not escape from closed chamber. This transmitted heat is represented by Q_{tg1} as shown in Fig. 3.28. The transmitted heat is given by

$$Q_{tg1} = I_r \times A \times t_g \times (1 - a_{ar}) \times t_g \tag{3.72}$$

where Q_{tg1}= Heat transmitted by the inner glass, I_r= Solar heat flux, A= Area of glass, t_g= Transmissivity of glass, a_{ar}= Absorptivity of argon gas.

The C23 is the compliance element which takes the flow *i.e.*, the heat flow and gives the effort *i.e.*, the temperature. This temperature can be detected by the effort detector (De) connected to 0_a-junction in the Bond Graph shown in Fig. 3.28.

$$K23 = \frac{1}{m_{air} \times C_{air}} \tag{3.73}$$

where $K23$= Capacitive element, m_{air}= Mass of air inside the cabin, C_{air}= Specific heat of air.

3.6.1 *Parameter Values*

Table 3.9: Parameter values for double layer glass cabin, argon flowing condition

Parameter	Value	Description
A	0.68 m^2	Area of glass
h_{air}	8 W/m^2-K	Convective heat transfer coefficient of air
h_{ar}	5.3 W/m^2K	Convective heat transfer coefficient of argon gas
e_{ar}	0.05	Emissivity of argon gas
e_{air}	0.01	Emissivity of air
σ	$5.67x10^{-8}$	Stefan Boltzmann Constant
m_{ar}	0.012095456 kg	Mass of argon gas
m_{air}	0.063 kg	Mass of air
C_{ar}	520 kJ/kg-K	Specific heat of argon gas
C_{air}	919 kJ/kg-K	Specific heat of air
m_g	23.4 kg	Mass of outer glass
m_{g2}	23.4 kg	Mass of inner glass
C_g	720 kJ/kg-K	Specific heat of glass
T_s	-261^0C	Temperature of space
e_g	0.9	Emissivity of glass
I_r	100 W/m^2	Heat flux
a_{ar}	0.1	Absorbtivity of argon
a_g	0.25	Absorptivity of glass
t_g	0.5	Transmissivity of glass
r_g	0.25	Reflectivity of glass
h_{ca}	10.25 W/m^2K	Convective heat transfer coefficient of glass

3.6.2 *Simulation Results*

The different parameters obtained by doing practical experiments, were used as the input to Bond Graph model of double layer glass with argon gas trapped as shown in Fig. 3.28. The parameters used as the input for the Bond Graph model were, atmospheric temperature, heat flux, various properties of toughened glasses, air and argon. The result obtained by the Bond Graph model of the double glass layer with argon flowing in between the two glasses is show in Fig. 3.29.

Table 3.10: Simulation results of double layer glass cabin, argon flowing condition

Sl. No.	T (Hour)	ST (^{0}C)	SRCCT (^{0}C)	SROGT (^{0}C)	SRIGT (^{0}C)	SRFAT (^{0}C)	Y (W/m^2)
1	0	36.5	36.5	36.5	36.5	36.5	
2	0.25	36.5	40.75	39.78	37.98	39.23	
3	0.5	36.8	42.67	41.98	39.9	41.28	
4	1	37.6	46.61	44.91	43.83	44.74	100
5	1.5	38.2	49.99	46.8	47.21	47.41	
6	2	38.9	53.05	48.48	50.27	49.82	
7	2.5	38.9	55.07	49.29	52.29	51.26	

where T= Time, ST= Surrounding Temperature, SRCCT= Simulation Results Central Cabin Temperature, SROGT= Simulation Results Outer Glass Temperature, SRIGT= Simulation Results Inner Glass Temperature, Y= Solar Heat Flux, SRATC= Simulation Results Flowing Argon Temperature.

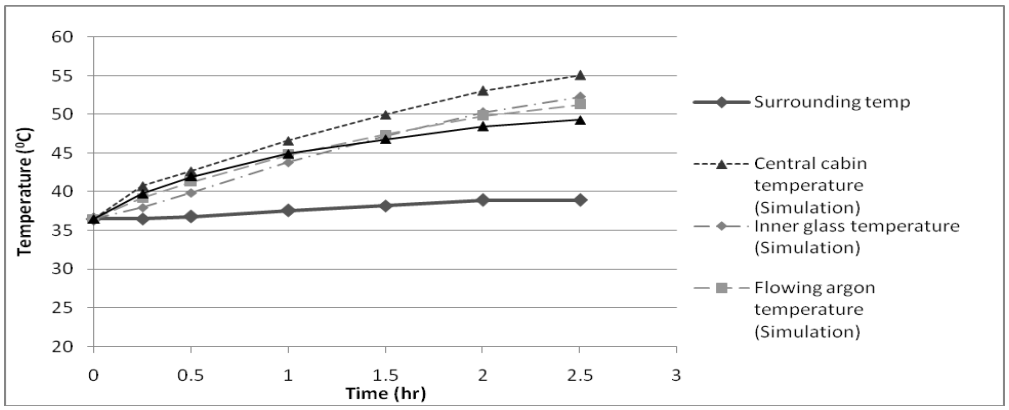

Fig. 3.29 Simulation results of double layer glass cabin with flowing argon

CHAPTER 4 EXPERIMENTAL PROCEDURE

4.1 Introduction

When a car is parked in direct sunlight, the heat waves in the form of electromagnetic wave from the sun enter into the passenger cabin of the vehicle. Heat waves enter into the compartment through windshield, side glass, roof material and the rear glass. As the heat waves passes through the glass, there is a change of wavelength of the heat waves. The wavelength of the electromagnetic waves increases as it pass through the glass, this electromagnetic waves of higher wavelength cannot escape outside the cars compartment. Thus the heat waves get trapped into the compartment which eventually increases the temperature of the car's interior compartment. The rise of temperature in the interior of the car is because of convection, radiation but radiation plays a major role in the heat accumulation in the interior of the car.

4.2 Selection of Material

This includes the materials which are being used and its properties. The materials used are wood, glass, thermocouple, thermometer, gas, pipe, T-connectors.

4.2.1 *Wood*

The wood is used as the supporting structure. A frame is made up of wood which acts as the supporting structure for the glass. The dimension of the frame was selected according to the availability of size of toughened glass. The dimension of the wooden frame is 411.6 mm × 411.6 mm × 649.6 mm.

All materials expand or contract on change of temperature. This expansion or the contraction decreases the strength of the material. For example steel, which is a non-combustible, if used in buildings, then it expands due to heat and results in collapse of the structure due to rise in temperature. The wood does not expands due to heat on the other hand it gains strength as it gets dried due to heat. The thermal conductivity of wood is also very low as compared to the other materials. The Aluminium transmits near about 7000 times the heat transmitted by wood, steal 1650 times and glass transmits 23 times the heat transmitted by wood. For this reason, wood is used for making the supporting structure of the toughened

glass. Ease of repairing and modification is one of the most important factors which motivate to use wood as supporting structure.

Fig. 4.1 Glass supporting structure

4.2.2 *Toughened Glass*

The toughened glass has far more resistance to breakage as compared to simple annealed glass and even if it breaks, it will break in a more predictable way. Toughened glass is made by treating annealed glass with a thermal tempering process. There is wide variety of glass such as laminated glass, annealed glass, coated glass, patterned glass, mirrored glass. Out of these glasses, laminated glass and the toughened glass are widely used in vehicles because of its non breaking tendency and even if it breaks, it break into small harmless pieces. The size of the toughened glass used was 310 mm × 548 mm × 5 mm Depending on this size the supporting structure was designed.

4.2.3 *Thermocouple and Digital Thermometer*

A thermocouple consist of two metals joined together to form two junctions. On one end the temperature is known and is considered as the reference temperature and on the other end temperature is unknown, this end could be hot or cold and its temperature is to be measured. Thus the thermocouple measures the unknown temperature of body with reference to the known temperature. As shown it consists of two dissimilar wires which are connected to each at junction P and Q. The P junction is at a temperature T1 and Q junction is at a temperature T2. As the two junctions are at different temperature, Peltier e.m.f is generated which is a function of temperature.

If the temperature of both the junctions is same, equal and opposite e.m.f will be generated at both junctions and the net current flowing through the junction is zero. If the two junctions are at different temperatures, the emf will not be equal to zero and there will be a net current flowing through the circuit. The total emf flowing through this circuit depends on the metals used within the circuit as well as the temperature of the two junctions. The device for measuring the current or emf is connected within the circuit of the thermocouple. It measures the amount of emf flowing through the circuit due to the two junctions of the two dissimilar metals maintained at different temperatures. Now, the temperature of the reference junctions is already known, while the temperature of measuring junction is unknown. The output obtained from the thermocouple circuit is calibrated directly against the unknown temperature. Thus the voltage or current output obtained from thermocouple circuit gives the value of unknown temperature directly.

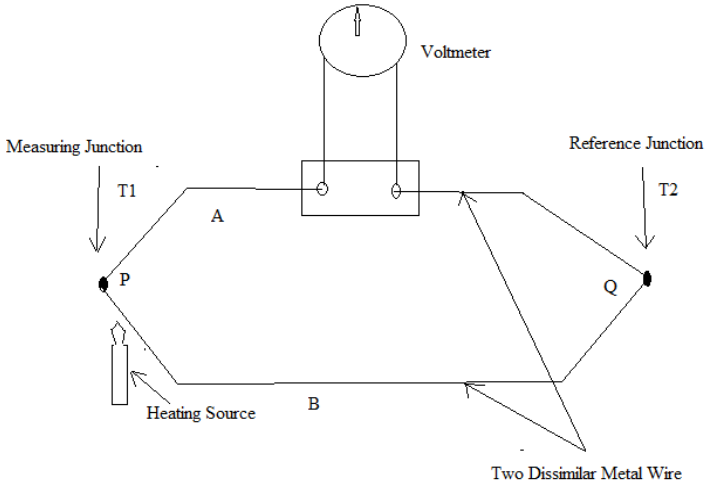

Fig. 4.2 Thermocouple

Fig. 4.3 Digital thermometer

4.2.4 *Argon Gas*

Argon is a noble gas and it lies in the 18^{th} group of the periodic table, it is the third most common gas present in the earth's atmosphere. Argon is widely used as shielding gas in welding and other industrial process for example argon shielding is used in graphite electric furnace for protecting the graphite from burning. Argon is odourless, colour less, non flammable and nontoxic as a solid, liquid, and gas. Argon gas has a low thermal conductivity and has insulating properties; it can also be used as a heat insulating gas.

Fig. 4.4 Argon gas cylinder

4.2.5 *Solar Power Meter*

Solar power meter is a device which is used to measure the solar heat flux coming from the sun. It indirectly measures the solar heat flux. It measures the solar heat intensity coming from the sun at any particular location and this value is further used to get the solar heat flux. The value obtained from the solar power meter is further substituted in the formula given below to get the solar heat flux. When the *Y i.e.,* solar heat flux is plotted against the *x i.e.,* solar intensity, the graph should be a straight line inclined at an angle of 45^0 and also the root mean square value should be equal to 1

$$Y=0.745x+1.839 \quad (4.1)$$

Fig. 4.5 Solar power meter

4.2.6 *Pipes and Connector*

Flexible foam pipes and connectors are used to connect all the compartments of dual glass as well as the gas cylinder. Different experiments were performed using different combination of glass layer and its gaseous medium. Experiment consists of analysis of single glass and double glass of the cabin which are filled with the atmospheric gas and argon gas alternatively. The complete experimental procedure for all combinations is explained in the following steps.

4.3 Experimentation on the System Surrounded by a Single Layer of Glass.

It is the first phase of the experiment; in this phase toughened glass having a dimension 548 mm × 310mm × 5mm is fitted into the wooden frame. The glass is properly sealed with the sealant so that no heat can escape from the assembly. Clay is used as a sealant for glass and the frame. The frame is insulated with thermocol from top and the bottom so that no heat could escape. The entire setup is exposed to the direct solar heat waves. The heat waves starts to accumulate in the interior of the cabin by means of conduction, convection and the radiation. Majority of the heat getting accumulated is due to the radiation. Two digital thermometers is used to measure cabin temperature and the atmospheric temperature and Solar power meter is used to measure the solar light intensity which will eventually give the value of the solar heat flux from the sun. The experiment starts at 11:00am on a hot sunny day of summer and readings are taken at an interval of 30 min from the start of the experiment.

Fig 4.6 Cabin made up of single glass layer

4.3.1 *Experimental Results*

The experiment was performed on 20th of May, 11:00 am onwards. Readings were taken at an interval of 30 minutes from the start of experiments. The results obtained are displayed in Fig. 4.7.

Table 4.1: Experimental results of single layer glass cabin

Sl.No.	Time (Hour)	Atmospheric Temperature (^{0}C)	Central Cabin Temperature (^{0}C)	Y(Mean) (W/m^2)
1	0	38	38	110
2	0.25	38	48	
3	0.5	39	53.4	
4	1	38.1	55.3	
5	1.5	38.2	56.2	
6	2	38.9	59	
7	2.5	39.1	59.4	

The atmospheric temperature is temperature of the environment, measured while taking the reading and the central cabin temperature is the temperature of the cabin were the heat waves are continuously getting accumulated due to the green house effect. Initially the temperature difference between the atmosphere and the cabin compartment is less, but as the time passes, this temperature difference goes on increasing. The temperature difference is shown graphically in Fig. 4.7.

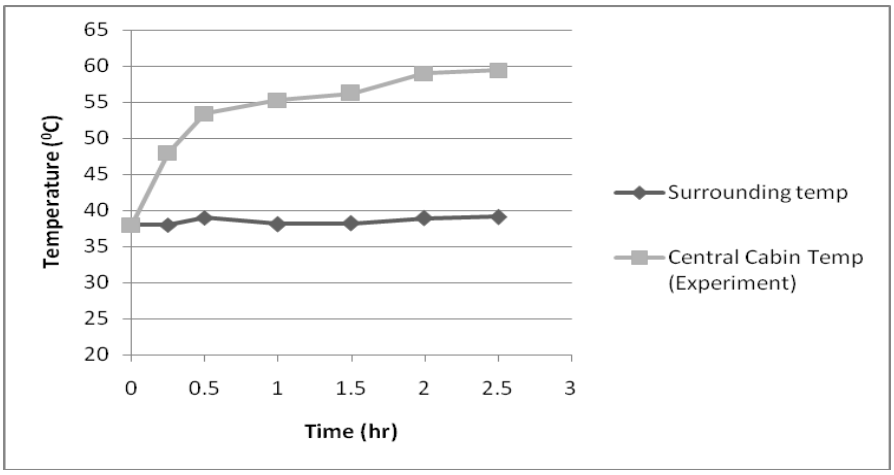

Fig. 4.7 Experimental results of single layer glass cabin

4.4 Experimentation on the System Surrounded by Double Layer of Glass with Air between Two Glasses.

In this phase of the experiment two toughened glasses having a dimension 548 mm × 310 mm × 5mm are used. These two glasses are assembled together in such a way that there is a gap of 10 mm in between the two glasses. For this purpose a separator is used which is having a thickness of 10mm, this separator is made up of wood and has a dimension 20 mm × 20mm × 10mm. Four pieces of such separator are placed at each corner of the glass and the other glass is placed over it so as to form an assembly. Further this double glass is sealed with a tape so that it becomes a single unit and prevents the leakage of air from the gap. In the similar fashion three more such assemblies are made which would be further fitted into the wooden frame and a cabin is prepared. The top and the bottom portion of the cabin are covered by thermocol sheet so that no heat could get escape. Two digital thermometers will used to measure the temperature in the interior of the cabin and the atmospheric temperature. Solar power meter will be used to measure the solar intensity which will eventually help in calculating the solar heat flux from the sun. This entire setup is placed in an open environment *i.e.*, in direct solar light. Due to the solar heat wave, the temperature in the

interior of the cabin will go on increasing and it will be measured by means of digital thermometer. Solar heat flux will be measured by means of the solar power meter.

The basic principle of such type of arrangement is to form a barrier for the heat flow. The toughened glass and the air which is trapped inside the two layers of glasses have a very less thermal conductivity thus it does not allow the heat waves to flow through it. Also as the density of the air is quite high, it makes propagation of the heat waves by convection quite difficult. The experiment starts at 11:00am on a hot sunny day of summer and readings are taken every 30 min from the start of the experiment.

Fig. 4.8 Double layer glass cabin with trapped air

4.4.1 *Experimental Results*

The experiment was performed on 19th of May, 11:00 am onwards. Readings were taken at an interval of 30 minutes from the start of experiment.

Table 4.2: Experimental results of double layer glass cabin, air trapped condition

Sl.No.	Time (Hour)	Atmospheric Temperature (^{0}C)	Central Cabin Temperature (^{0}C)	Y(Mean) (W/m^2)
1	0	36.5	36.5	
2	0.25	36.5	41.6	
3	0.5	37.3	47.1	
4	1	37.4	49.9	118
5	1.5	38.1	51	
6	2	38	53.4	
7	2.5	38.8	57.4	

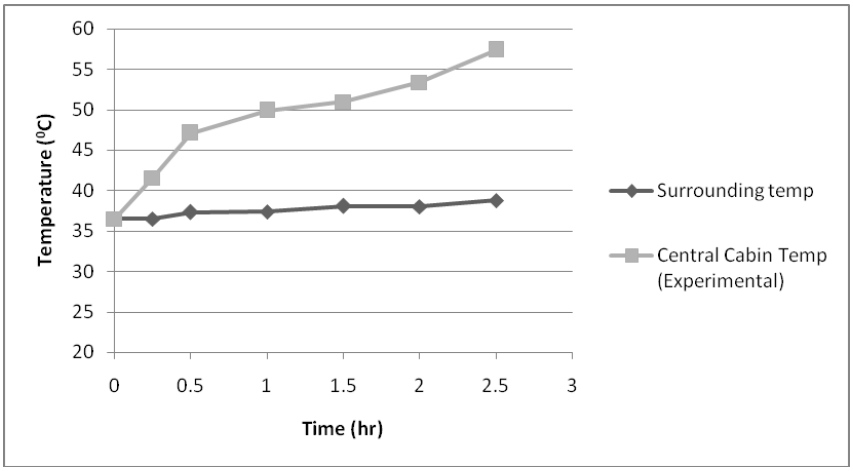

Fig. 4.9 Experimental results of double layer glass with trapped air.

As shown in Fig 4.9, atmospheric temperature has a variation of about 2^0C to 3^0C *i.e.*, it can be said that there is not much variation in the atmospheric temperature. But the central cabin temperature goes on increasing. Initially the temperature difference between the central cabin temperature and the atmospheric temperature was less but with the time this temperature difference went on increasing. But when compared to the Fig. 4.7, *i.e.*, experiment performed on the single layer glass, the temperature difference obtained in the double glass was quite less than that of the single glass.

4.5 Experimentation on the System Surrounded by Double Layer of Glass with Argon between Two Glasses.

The experiments performed is similar to that of performed in the double glass with the air trapped in between the glasses, only the difference is that instead of the air, argon is used as the insulating gas. As the argon gas is having a low thermal conductivity therefore it does not allow the heat to conduct through it. Also as the argon is trapped *i.e.*, no movement of the argon, there is no heat flow by convection. Due to the inert nature of argon, it does not involves in any type of the chemical reactions and also it does not create any hazards on the humans and animals. Argon is odourless, colour less, non flammable and nontoxic in all phase of solid, liquid, and gas.

Fig 4.10 Glass separated by separator

As explained earlier in the air trapped condition, a separator is used in the argon trapped condition. To avoid the leakage of the argon gas, a through hole of 3 mm is drilled through separator. Further this separator is again positioned at each corner of the glass so as to create a gap of 10 mm in between the two toughened glasses. Now the two toughened glass along with the separator in between the two acts as the single unit, it is then sealed from all four sides by means of a sealing tape. A pipe of 3 mm diameter is inserted through the hole of the separator and this pipe is further connected to the argon gas cylinder. This assembly is prepared so as to avoid the leakage of the argon gas and the argon gas can be trapped in between the gap of two glasses. Argon gas is then released from the cylinder so that it can be filled in the space between the two glasses. Constant flow of argon gas is maintained in all the four double layer glass assemblies so that atmospheric gas is displayed by the pressurised

argon gas. Constant flow is checked by counting the bubbles coming out from the outlet pipe which is dipped in water. When the bubble count per unit time is stabilised then argon gas flow is stopped.

The displacement of the atmospheric gas by pressurise argon gas is also verified by a parallel arrangement installed during the experiment. In this arrangement outlet line is made to pass through a closed chamber having a burning candle inside it. The candle stops burning as soon as there is no oxygen available in the outlet pipe coming out from the double layered glass assemblies. Whole process is demonstrated in Fig. 4.11.

Fig. 4.11 Argon-oxygen separator

When the pressure at the supply and at the outlet of the assembly of the glasses becomes equal, it means that the argon gas has been completely filled in the gap of the two glasses. At this point both supply and the exit of the argon gas are closed by means of the hand tape wall and this entire setup is exposed to the solar heat so as to check the amount of heat getting accumulated inside the setup.

As explained in the earlier phase of the experimentation, digital thermometer and thermocouple will be used to measure the temperature generated in the interior of the cabin and the atmospheric temperature. Solar power meter will be used to measure the solar intensity which will eventually help in calculating the solar heat flux from the sun. The experiment starts at 11:00am on a hot sunny day of summer and readings are taken every 30 min from the start of the experiment.

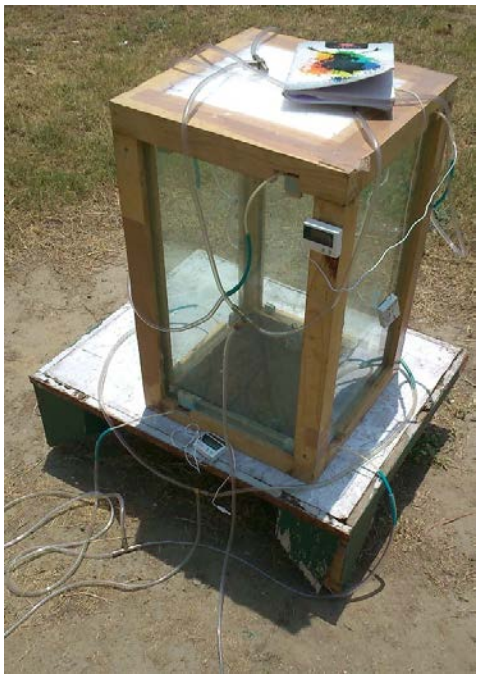

Fig. 4.12 Cabin of double glasses with trapped argon.

4.5.1 *Experimental Results*

The experiment was performed on 8th of May 11:00 am onwards. Readings were taken at an interval of 30 minutes from the start of experiment.

Table 4.3: Experimental results of double layer glass cabin, argon trapped condition

Sl.No	Time (Hour)	Atmospheric Temperature (^{0}C)	Central Cabin Temperature (^{0}C)	Y(Mean) (W/m^2)
1	0	36	36	100
2	0.25	36	41	
3	0.5	38	47.8	
4	1	39.1	51	
5	1.5	39.5	51.6	
6	2	39.4	54	
7	2.5	40.4	57.1	

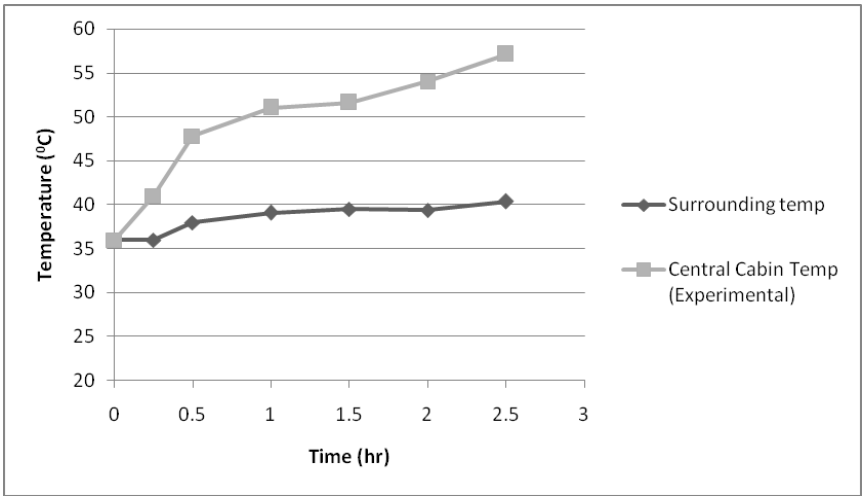

Fig. 4.13 Experimental results of double layer glass cabin with trapped argon.

The atmospheric temperature ranges between 36^0C to 40.4^0C but the rise in temperature of the central cabin is quite high *i.e.*, close to 60^oC. This rise in temperature is very much unbearable. But compare to the results obtained by single glass cabin and double layer glass, air trapped condition, this rise in temperature is very much low. The rise in temperature has fallen by nearly 3^0C. This has been possible because of the argon gas used, as the thermal conductivity of the gas is low and the trapping condition makes the heat transfer by convection very difficult. This gas is not capable to reduce the heat transfer by radiation, so the main reason of rise in temperature is due to the radiation heat flow.

4.6 Experimentation on the System Surrounded by Double Layer of Glass with Flowing Argon between Two Glasses.

The entire setup is similar to that of the prepared for the argon trapped condition, only the difference is that argon gas will not be trapped in between the glasses but it will be allowed to flow continuously. The entire setup was placed into the direct sunlight so as to check the effect of the solar heat on the interior of the cabin.

Fig. 4.14 Cabin of double glasses with flowing argon.

4.6.1 *Experimental Results*

The experiment was performed on 9th of May 11:00 am onwards. Readings were taken at an interval of 30 minutes from the start of experiment.

Table 4.4: Experimental results of double layer glass cabin, argon flowing condition

Sl.No.	Time (Hour)	Atmospheric Temperature (^{0}C)	Central Cabin Temperature (^{0}C)	Y(Mean) (W/m^2)
1	0	36.5	36.5	100
2	0.25	36.5	42	
3	0.5	36.8	47	
4	1	37.6	50	
5	1.5	38.2	51	
6	2	38.9	53	
7	2.5	37.9	55	

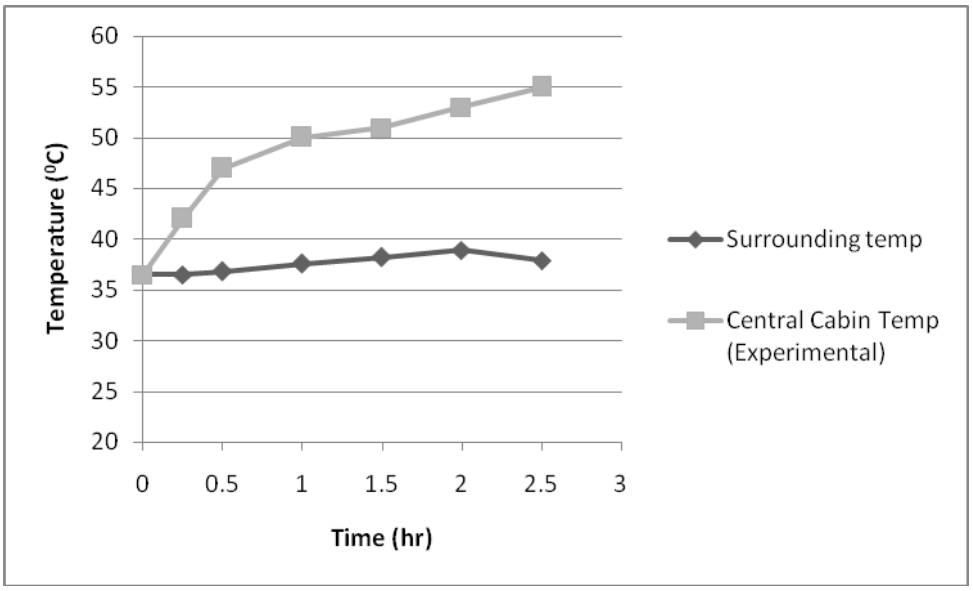

Fig. 4.15 Experimental results of double layer glass cabin with flowing argon.

As shown in the Fig. 4.15, the temperature difference between central cabin temperature and atmospheric temperature is less as compared to the single glass layer and the double glass with air trapped but nearly same to that of double glass with argon trapped. The reason behind this could be that argon is continuously flowing through the double glass. This flowing will increase heat transfer by convection through gas and thus eventually result in the decrease in temperature of the compartment.

4.7 Validation with Theoretical Results

The results obtained by the experimental process are further validated by means of the software called as the bond graph. The results obtained by the bond graph and by the experiment are nearly same.

4.7.1 *Validation of Single Layer Glass Cabin*

The results obtained by the experiment and by the bond graph are shown in the Table 4.5 and the Fig. 4.16.

Table 4.5: Results of single layer glass cabin

Sl.No.	T (Hour)	ST (^{0}C)	ERCCT (^{0}C)	SRCCT (^{0}C)	SRGT (^{0}C)	Y (W/m^2)
1	0	38	38	38	38	110
2	0.25	38	48	50.3	43.5	
3	0.5	39	53.4	54.66	47.9	
4	1	38.1	55.3	56.6	49.78	
5	1.5	38.2	56.2	57.48	50.66	
6	2	38.9	59	58.6	51.8	
7	2.5	39.1	59.4	59.4	52.58	

where T= Time, ST= Surrounding Temperature, ERCCT= Experiment results central cabin temperature SRCCT= Simulation Results Central Cabin Temperature, SRGT= Simulation Results Glass Temperature

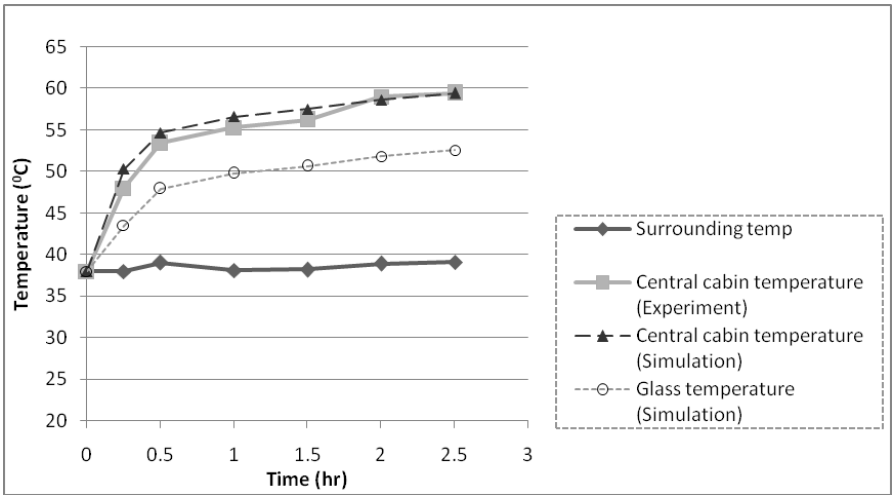

Fig. 4.16 Experimental results v/s simulation results of single layer glass

As show in the Fig. 4.16, the results obtained by doing practical experiments and by bond graph aproach is nearly same. As shown in the Fig. 4.16, the graph of central cabin

temperature obtained by the experiment results moves close parallel to that of the graph obtained by the simulation results.

4.7.2 *Validation of Double Layer Glass Cabin with Air in between Two Glass*

The results obtained by the experiment and by the simulation software (bond graph) are shown in the Table 4.6 and the Fig. 4.17.

Table 4.6: Results of double layer glass, air trapped condition

Sl.No.	T (Hour)	ST (^{0}C)	ERCCT (^{0}C)	SRCCT (^{0}C)	SROGT (^{0}C)	SRIGT (^{0}C)	SRTAT (^{0}C)	Y (W/m^2)
1	0	36.5	36.5	36.5	36.5	36.5	36.5	
2	0.25	36.5	41.6	41.8	40	38.2	39.1	
3	0.5	37.3	47.1	44.5	42.9	40.9	41.9	
4	1	37.4	49.9	48.2	45.1	44.6	44.9	118
5	1.5	38.1	51	52	47	48.4	47.7	
6	2	38	53.4	54.4	47.8	50.8	49.3	
7	2.5	38.8	57.4	57.3	49.3	53.7	51.6	

where T= Time, ST= Surrounding Temperature, ERCCT= Experiment result central cabin temperature, SRCCT= Simulation Results Central Cabin Temperature, SROGT= Simulation Results Outer Glass Temperature, SRIGT= Simulation Results Inner Glass Temperature, Y= Solar Heat Flux, SRATC= Simulation Results Air Trapped Temperature.

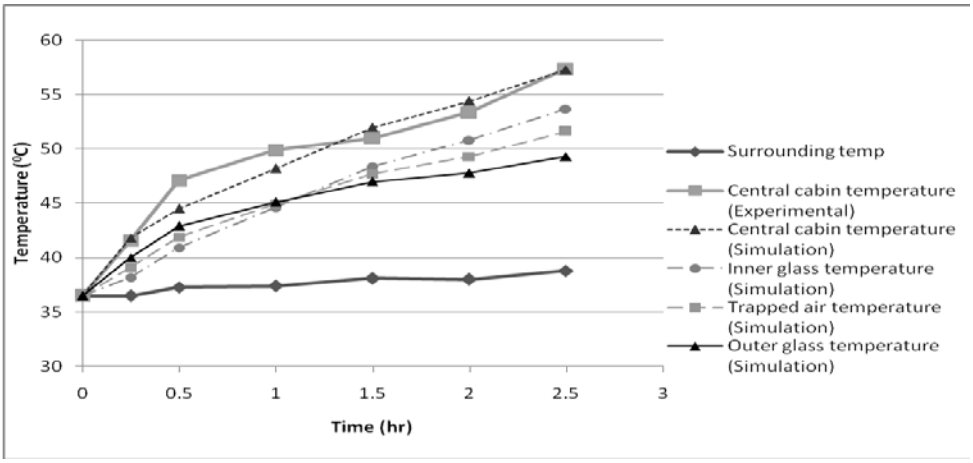

Fig. 4.17 Experimental results v/s simulation results of double layer glass with trapped air.

4.7.3 *Validation of Double Layer Glass Cabin with Argon in between the Two Glasses*

The results obtained by the experiment and by the simulation software (bond graph) are shown in the Table 4.7and the Fig. 4.18.

Table 4.7: Results of double layer glass cabin, argon trapped condition

Sl.No.	T (Hour)	ST (^{0}C)	ERCCT (^{0}C)	SRCCT (^{0}C)	SROGT (^{0}C)	SRIGT (^{0}C)	SRTAT (^{0}C)	Y (W/m^2)
1	0	36	36	36	36	36	36	100
2	0.25	36	41	40.25	39.34	37.47	38.68	
3	0.5	38	47.8	43.86	43.49	41.09	42.52	
4	1	39.1	51	48.18	47.11	45.41	46.56	
5	1.5	39.5	51.6	51.52	48.88	48.74	49.25	
6	2	39.4	54	53.95	49.52	51.17	50.95	
7	2.5	40.4	57.1	57.08	51.26	54.3	53.5	

where T= Time, ST= Surrounding Temperature, ERCCT= Experimental result central cabin temperature, SRCCT= Simulation Results Central Cabin Temperature, SROGT= Simulation

Results Outer Glass Temperature, SRIGT= Simulation Results Inner Glass Temperature, Y= Solar Heat Flux, SRTAT= Simulation Results Trapped Argon Temperature.

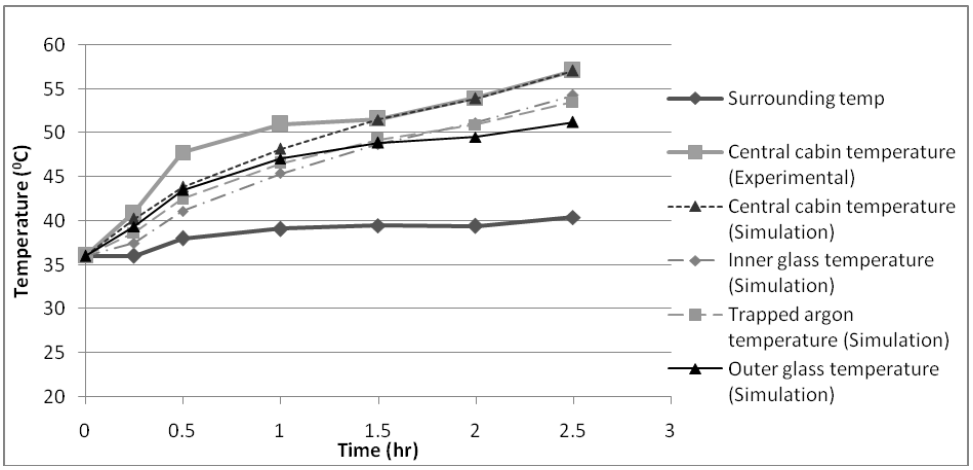

Fig. 4.18 Experimental results v/s simulation results of double layer glass with trapped argon.

4.7.4 *Validation of Double Layer Glass Cabin with Argon in between the Two Glass*

The results obtained by the experiment and by the simulation software (bond graph) are shown in the Table 4.8 and the Fig. 4.19.

Table 4.8: Results of double layer glass cabin, argon flowing condition

Sl.No.	T (Hour)	ST (^{0}C)	ERCCT (^{0}C)	SRCCT (^{0}C)	SROGT (^{0}C)	SRIGT (^{0}C)	SRFAT (^{0}C)	Y (W/m^2)
1	0	36.5	36.5	36.5	36.5	36.5	36.5	
2	0.25	36.5	42	40.75	39.78	37.98	39.23	
3	0.5	36.8	47	42.67	41.98	39.9	41.28	
4	1	37.6	50	46.61	44.91	43.83	44.74	100
5	1.5	38.2	51	49.99	46.8	47.21	47.41	
6	2	38.9	53	53.05	48.48	50.27	49.82	
7	2.5	38.9	55	55.07	49.29	52.29	51.26	

where T= Time, ST= Surrounding Temperature, SRCCT= Simulation Results Central Cabin Temperature, SROGT= Simulation Results Outer Glass Temperature, SRIGT= Simulation Results Inner Glass Temperature, Y= Solar Heat Flux, SRATC= Simulation Results Flowing Argon Temperature.

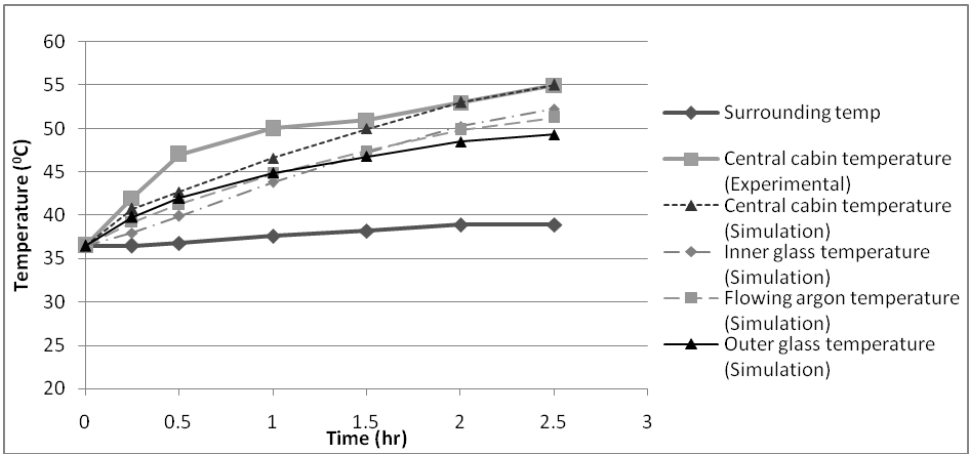

Fig. 4.19 Experimental results v/s simulation results of double layer glass with flowing argon.

CHAPTER 5 CONCLUSION

5.1 Conclusion

The main objective of this thesis was to check and reduce the amount of heat getting accumulated in the interior cabin of a vehicle. So, for this process a closed cabin of toughened glass was made and experiments were performed on this closed cabin to check the amount of heat getting accumulated into the interior of the vehicle. The aim was achieved by adopting the following methods.

- A closed cabin of single layer toughened glass was placed in direct sunlight so as to check the amount of heat getting accumulated into the closed cabin. The rise in temperature of the air present inside the closed cabin was very high. It gives an idea of the rate at which heat gets accumulated into the cabin of actual vehicle.
- On replacing the single layer toughened glass with double layer toughened glass cabin with air in between the two glasses, it was seen that the rate of rise of temperature of the air present inside the cabin was reduced. This reduction in temperature was because of the insulating property of the air.
- In the third phase of the experiment, only the air is replaced with the argon gas *i.e.*, argon will be trapped in between the two glasses. It was observed that the temperature of the air present inside the closed cabin was reduced by a greater extent. This reduction of heat was due to low thermal conductivity of the argon gas.
- The argon which was trapped in third phase of experiment was now allowed to flow in between the two layers of glasses. The rate of heat accumulation inside the compartment was still reduced further. But this reduction of heat was nearly same as that of reduction of heat obtained by trapping the argon gas in between the two glasses.

5.2 Scope of Future Work

Based on this thesis, the following areas of work are suggested for further exploration.

- Work can be done on the roof material of the vehicle so as to stop the heat accumulation in the interior of the vehicle.
- Work can be done on the interior materials of the vehicle.

REFERENCES

[1] Ismail, K.A.R., Salinas, T., and Henriquez, J.R. Comparison between PCM filled glass window and absorbing gas filled windows. *Energy and Building*, 2008, **40**, 710–719.

[2] Durrani, S.M.A., Khawaja, E.E., Al-Shukri, A.M., and Al- Kuhaili M.F. Dielectric/Ag/dielectric coated energy-efficient glass window for warm climates. *Energy and Building*, 2004, **36**, 891–898.

[3] Chen, X., Lv, Q., and Yi, X. Smart window coating based on nanostructured VO_2 thin film. *Elsevier Publication*, 2012, **123**, 1187−1189.

[4] Tonooka, K., and Kikuchi, N. Super-hydrophilic and solar-heat-reflective coating for smart windows. *Thin Solid Films*, 2013, **532**, 147−150.

[5] Nagamedianova, Z., Ramirez-Garcia, R.E., Flores-Arevalo, S.V., Miki-Yoshida, M., and Arroyo-Ortega, M. Solar heat reflective glass by nanostructured sol-gel multilayer coatings. *Optical Material*, 2011, **33**, 1999−2005.

[6] Zhang, H., Dai, L., Xu, G., Li, Y., Chen, W., and Wen-Quan, T. Studies of air-flow and temperature fields inside a passenger compartment for improving thermal comfort and saving energy. Part I: Test/numerical model and validation. *Applied Thermal Engineering*, (2009), **29**, 2022–2027

[7] Jamekhorshid, A., and Sadramel, S.M., Application of Phase Change Materials (PCMs) in Maintaining Comfort Temperature inside an Automobile. *World Academy of Science, Engineering and Technology*, 2012, **06**, 01−25.

[8] Risberg, J., and Hope, A. Thermal insulation properties of argon used as a dry suit inflation gas. Norwegian Underwater Institute and Royal Norwegian Navy, Berger, Norway.

[9] Xamána, J., Pérez-Nucamendia, C., Arcea, J., Hinojosab, J., Álvareza, G., and Zavala-GuillénaaCentro, I. Thermal analysis for a double pane window with a solar control film for using in cold and warm climate. *Energy and Buildings*, 2014, **76**, 429–439.

[10] Mezrhab, A., and Bouzidi, M. Computation of thermal comfort inside a passenger car compartment. *Applied Thermal Engineering*, 2006, **26**, 1697–1704.

[11] Mazzoni. Reducing Solar Radiation Transmittance of Installed Glazing. US Patent, Application no 710031, Aug. 16, 1977, 4,041663.

[12] Hussain Al-Kayiem, H., Firdaus, B.M., Sidik, M., and Yuganthira, R.A., Munusammy, L. Study on the Thermal Accumulation and Distribution Inside a Parked Car Cabin. *American Journal of Applied Sciences*, 2010, **7(6)**, 784−789.

[13] Kaynakli, O., and Kilic, M. An investigation of thermal comfort inside an automobile during the heating period. *Applied Ergonomics*, 2005, **36**, 301–312.

[14] Zhang, H., Dai, L., Xu, G., Li, Y., Chen, W., and Wen-Quan, T. Studies of air-flow and temperature fields inside a passenger compartment for improving thermal comfort and saving energy. Part II: Simulation results and discussion. *Applied Thermal Engineering*, (2009), **29**, 2028–2036.

[15] Dadour, I. R., Almanjahie, I., Fowkes, N. D., Keady, G., and Vijayan K. Temperature variations in a parked vehicle. *Forensic Science International*, 2011, **207**, 205–211.

[16] Lee, J. W., Jang, E. Y., Lee, S. H., Ryou, H. S., Choi, S., and Kim Y. Influence of the spectral solar radiation on the air flow and temperature distributions in a passenger compartment. *International Journal of Thermal Sciences*, 2014, **75**, 36−44.

[17] Sanaye, S., Dehghandokht, M., Fartaj, A. Temperature control of a cabin in an automobile using thermal modelling and fuzzy controller. *Applied Energy*, 2012, **97**, 860–868.

[18] Alahmer, A., Mayyas, Omar, A., Shan, D. Vehicular thermal comfort models; a comprehensive review. *Applied Thermal Engineering*, 2011, **31**, 995-1002.

[19] François, E.C., and Nebot, A. The Modelica Bond Graph Library.

[20] François, E.C., and Greifeneder, J. Object-Oriented Modeling of Convective Flows Using the Dymola Thermo-Bond-Graph Library.

[21] Weiner, M., and François, E.C. Modelling and Simulation of a Solar Energy System by use of Bond Graph.

[22] Greifeneder, J., and François, E.C. Modelling Convective Flow Using Bond Graph.

[23] Hassan, S. A., Thesis on fundamentals studies of passive, active and semi active automotive suspension system, 1986.

[24] Reimpell, J., Stoll, H., and Betzler, J., The automotive Chassis, *Engineering Principles*, Second Edition, **34**, 2001, 73–85.

CURRICULUM VITAE

Sushank Dixit did his graduation from P.E.S College of Engineering in Bachelor of Mechanical Engineering (B.E), in the year 2010. After that he has worked as Graduate Trainee Engineer in Aurangabad Electrical Limited, District-Aurangabad, Maharashtra in the year 2010–2011. In the year 2012, he joined in the Master of Engineering (CAD/CAM Engineering) Programme at Thapar University, Patiala, Punjab. His ME thesis work is in the area of Automobiles as Modelling and Experimental Analysis of a Thermal System Equivalent to a Car Parked in Direct Sunlight. A journal paper is under preparation.